Tijdschrift van het NERG

DE VERENIGING NERG

Het NERG is een wetenschappelijke vereniging die zich ten doel stelt de kennis en het wetenschappelijk onderzoek op het gebied van de elektronica, signaalbewerking, communicatie- en informatietechnologie te bevorderen en de verbreiding en toepassing van die kennis te stimuleren.

BESTUUR

prof.dr.ir. W.C. van Etten, voorzitter
prof.dr.ir. P. Regtien,
    vice-voorzitter
ir. E. Bottelier, secretaris
P.F. Maartense, penningmeester
dr.ir. A.B. Smolders,
    tijdschrift-manager
dr.ir. Tj.J. Tjalkens,
    programma-manager
ir. R.J. Kopmeiners, web-beheer
vacature, onderwijs-commissaris
vacature, ledenwervings-manager

LIDMAATSCHAP

Voor het lidmaatschap wende men zich via het correspondentie-adres tot de secretaris of via de NERG website: http://www.nerg.nl. Het lidmaatschap van het NERG staat open voor hen, die aan een universiteit of hogeschool zijn afgestudeerd en die door hun kennis en ervaring bij kunnen dragen aan het NERG. De contributie wordt geheven per kalenderjaar en is inclusief abonnement op het Tijdschrift van het NERG en deelname aan vergaderingen, lezingen en excursies.

De jaarlijkse contributie bedraagt voor gewone leden € 43,- en voor studentleden € 21,50. Bij automatische incasso wordt € 2,- korting verleend. Gevorderde studenten aan een universiteit of hogeschool komen in aanmerking voor het studentlidmaatschap. In bepaalde gevallen kunnen ook andere leden, na overleg met de penningmeester voor een gereduceerde contributie in aanmerking komen.

HET TIJDSCHRIFT

Het tijdschrift verschijnt vijf maal per jaar. Opgenomen worden artikelen op het gebied van de elektronica, signaalbewerking, communicatie- en informatietechnologie. Auteurs, die publicatie van hun onderzoek in het tijdschrift overwegen, wordt verzocht vroegtijdig contact op te nemen met de hoofdredacteur of een lid van de Tijdschriftcommissie.

Toestemming tot overnemen van artikelen of delen daarvan kan uitsluitend worden gegeven door de tijdschriftcommissie. Alle rechten worden voorbehouden.

TIJDSCHRIFTCOMMISSIE

INHOUD

Van de redactie

Huib Visser
Hoofdredacteur
visser@ieee.org

Het vierde nummer van jaargang 67 moet helaas weer beginnen met een droevig bericht. Voor de tweede keer in korte tijd heeft het NERG afscheid moeten nemen van een gewaardeerd actief lid. Op 21 november 2002 is, veel te vroeg, Oscar Rikkert de Koe overleden. Oscar is zonder meer een markant en bijzonder actief lid van het NERG geweest. Hoewel hij geen bestuursfunctie meer vervulde het afgelopen jaar, zal zijn kennis, ervaring en behulpzaamheid bijzonder gemist worden. Op de laatste pagina's van dit nummer van het Tijdschrift staan Wim van Etten, Bob van Loon en Gerard Havermans uitgebreider hierbij stil. Op deze plaats willen we, namens de redactie, Oscar's familie sterkte wensen met het geleden verlies.

Dit nummer van het Tijdschrift alsmede een deel van het komende nummer zal in het teken staan van de "25th ESA Antenna Workshop on Satellite Antenna Technology", welke 18 tot en met 20 september 2002 plaatsvond bij ESTEC te Noordwijk. Deze workshop werd georganiseerd in samenwerking met - mede - het NERG. In dit en het komende nummer van het Tijdschrift zullen we daarom de Nederlandse bijdragen, zoals deze in de proceedings van de Workshop te vinden zijn, de revue laten passeren. Kees van 't Klooster, voorzitter van deze workshop, alsmede Maurice Paquay en Margreet van der Plas, allen werkzaam bij ESTEC, worden bedankt voor hun hulp bij het aanleveren van de bijdragen.

In het kader van "Satellite Antenna Technology" treft u - wellicht tegen de verwachting in - een grote diversiteit aan antenne-gerelateerde artikelen aan. Achtereenvolgens komen aan bod: " Het meten van millimetergolf-antennes, grote antennes in de ruimte, miniatuur-antennes, een model voor een Cosmic Microwave Background polarimetrische telescoop en een semi-actieve Ka-band reflec-tarray. In het volgende nummer van het Tijdschrift zullen de overige Nederlandse bijdragen aan deze, mede door het NERG mogelijk gemaakte, workshop aan bod komen.

Rest mij nog om - zij het met enige terughoudendheid - u, namens de redactie, een prettige kerst en een voorspoedig 2003 toe te wensen. Met enige terughoudendheid, want ik realiseer mij dat, hoewel het midden december 2002 is dat ik dit schrijf, u dit waarschijnlijk leest halverwege januari 2003. Het zal u niet ontgaan zijn dat het verschijnen van het Tijdschrift onregelmatig geworden is. Dit is het gevolg van het feit dat het uitbrengen van het Tijdschrift door een kleine groep mensen gedragen wordt. Ziekte van één van deze mensen heeft dan direct een vertraging tot gevolg. Als redactie proberen we dit zo goed mogelijk op te vangen, maar het is niet te voorkomen dat u als lezer hier iets van merkt. Ik denk dat er niets anders op zit dan dit te accepteren in deze tijd van afnemende interesse voor actief bijdragen aan het verenigingsleven.

Millimeter-wave front-end instrumentation for the ESTEC compact antenna test range.

M.H.A. Paquay, D.R. Vizard, D. Korneev, P. Ivanov, V.J. Vokurka

Abstract
In preparation of antenna testing for future space exploration missions, ESA ESTEC decided to upgrade its Compact Antenna Test Range into the mm-wave region. As a goal, the same functionality as at lower frequencies should be realized. That means: full (octave) frequency band coverage, sweep or step frequency capability, high dynamic range in the order of 70-80 dB, computer controllable and compatibility with the existing HP8530 receiver equipment. The 110 - 170 GHz band was chosen as a first step to test the concept. With a transmitter, based on a PLL-locked Backward Wave Oscillator, and a receiver based on sub-harmonic mixing in combination with multiplexing of the LO, a system was created with unsurpassed performance in terms of band coverage and dynamic range.

Introduction
Mankind, or at a least part of the scientific community, always wanted to know what happened at the beginning of time, how galaxies were formed in the early universe, how stars were and are formed, in order to get a clue how the earth became what it is now. Traces can be found as emissions from stars or small perturbations of the cosmos. Other scientists study the processes taking place in the atmosphere of the earth as it is today. Study of the spectral absorption lines of chemicals like H_2O, CO_2, O_2, O_3 etc can tell us a lot about processes like the greenhouse effect or ozone depletion.

Many of these effects take place in the millimetre and sub-millimetre wave region of the spectrum. Several Earth observation instruments and astronomical missions, like Planck, Herschel, Master and Achechem [1], equipped with instruments operating on these frequencies, are being planned and developed by ESA. The design and manufacturing of these instruments is a challenge of its own. However, at the end the performance has to be verified by measurements so test techniques and instrumentation have to keep up with these developments.

Most of the instruments operate in a few narrow bands, for example the spectral absorption lines of certain chemicals. On the other hand, remote sensing instruments are designed for the "windows" were there is minimal absorption. All of these instruments can be based on narrow band components, like e.g. Gunn oscillators, however a test engineer, faced with the combined requirements of all the instruments will prefer a wideband coverage and easy tunability.

ESA-ESTEC decided to upgrade its Compact Antenna Test Range instrumentation into the mm-wave region. As a goal, the same functionality as at lower frequencies should be realized. That means: full (octave) band coverage, sweep or step frequency capability, coherent measurement of amplitude and phase, high dynamic range in the order of 70 to 80 dB, computer controllable and preferable compatible with existing receiver equipment (HP8530). The 110-170 GHz band (sometimes denoted as D-band) was chosen as a first step to test the concept. Further upgrades, up to 350 GHz, are foreseen if the quality of the Quiet Zone, mainly determined by the (unknown) surface profile of the Compact Antenna Test Range reflectors, remains acceptable.

System design considerations
When passing the 100 GHz border, the RF engineer will notice that he has entered a new zone were a term like "standard catalogue item" fades away. Nevertheless, a good starting point for the design is still the power budget.

Starting at the receiver end, it is clear that there is no equipment that can do coherent measurements at mm-wave frequencies. The signal has to be down-converted to a (standard) measurable frequency. These receivers, e.g. an HP8511, have a

minimum detectable power of about –110 dBm. Taking into account the cables losses between mixer and receiver (> 5 dB), the conversion loss of the harmonic mixer (15-20 dB for sub-harmonic mixing, 30-50 dB for high harmonic numbers) and the free space loss in a Compact Antenna Test Range (including the gains of range feed and AUT: 10-15 dB), the conclusion is that the minimum available output power of the transmitter should be 0 dBm. So besides the requirements, mentioned in the introduction, the dynamic range requirement translates to:

- Transmit power: minimum 0 dBm
- Low receiver conversion loss

The system can be divided in three major components: the transmitter, the receiver front-end and the range feed antenna.

The transmitter.
There are a number of sources available for generating output power at mm-wave frequencies. A good overview is given by Zimmermann [2]. Synthesizers are not in his list for obvious reasons. Commercial available synthesizers stop at about 50 GHz. HP/Agilent offers frequency extensions up to 110 GHz by means of multipliers (HP83557-8). Above that, Oleson Microwave Labs (OML) offers HP-compatible multiplier sources [3], however the multiplication number to be used reduces the efficiency and the output power does not match the required 0 dBm.

Other popular sources are the GUNN-oscillators. They are frequently used in instruments with narrow banded operation. Their main limitation is their tunability. Mechanical tuning is not the preferred solution for a measurement range and electrical tuning is limited to about 5%. Every AUT would require the purchase of a dedicated GUNN-oscillator front-end.

Solid-state sources are emerging, however, their output power is still very limited.

The Backward Wave Oscillator (BWO, also known as carcinotron) combines both the requirements of output power and tunability. The main drawbacks are that it is a tube with a limited lifetime (typical 2000 hrs) requiring high voltage supply. Another drawback is the phase noise and stability of this source. Since the oscillator frequency is voltage controlled, any ripple (e.g. 50 Hz) will cause a frequency modulation. Recently, there have been some developments: ELVA-1 [4], supported by FARRAN Technology Ltd. [5], has developed a BWO-based Millimetre Wave Generator with integrated power supply and control unit.
Säily reported about a BWO, phase locked to an external source to improve the phase noise [6] Combination of these two developments yields a promising concept as pictured in figure 1. To get sufficient bandwidth for the PLL, the reference frequency is set to 300 MHz.

The reference frequency for the PLL and the LO are externally supplied.

The receiver front-end.
On the receiver side, the most obvious choice for down-mixing the millimetre wave frequency is a harmonic mixer. The only freedom of choice is the harmonic number, and connected to that, the LO-frequency. Keeping in mind that this concept should be expandable to 350 GHz with an LO below 40 GHz, the harmonic number should be at

Figure 1: Transmit part: a phase-locked BWO.
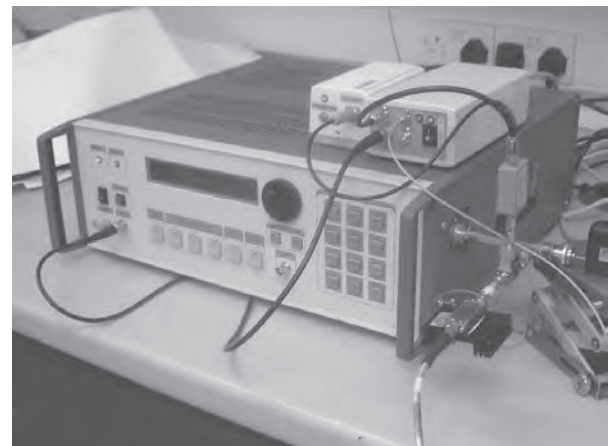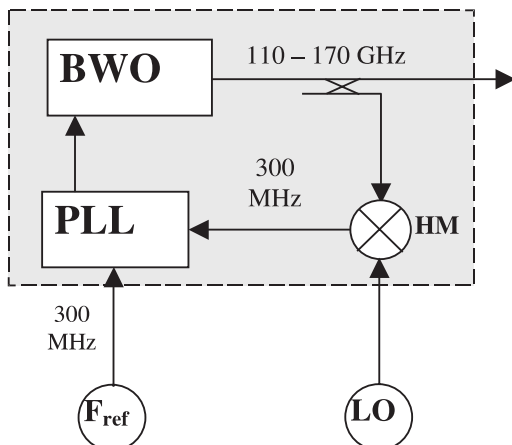
Figure 2: Receiver front-end

least 9. With these high harmonic numbers, the conversion loss is in the order of 30 dB. Compared to the 15 dB as assumed in the power budget of the introduction, this would reduce the dynamic range by 15 dB.

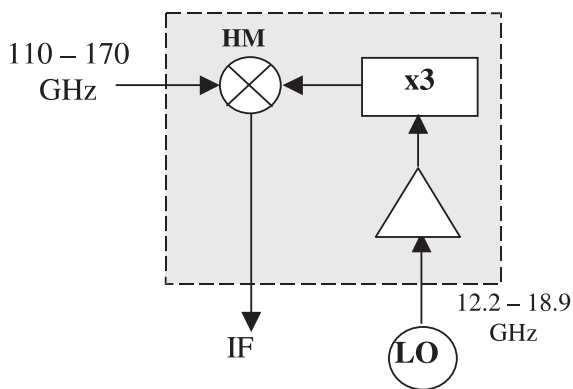The only solution to keep the conversion losses to 15 dB is the use sub-harmonic mixing with a harmonic number of 3 in combination with a multiplication of the LO frequency by a factor 3. This combination was available by ELVA-1 as their model DC-THM/9-06-N. Figure 2 shows the receiver front-end, with an extra LNA in the IF line.

System design

For the system design, choices have to be made for the harmonic number N on the transmit side and the IF to be fed into the receiver. On the transmit side, the relation between the frequencies is:

$$F_{BWO} = N * LO_1 + F_{ref} = N * LO_1 + 300 \text{ MHz} \quad (1)$$

On the receive side, the frequency relation is:

$$F_{BWO} = 9 * LO_2 + IF \quad (2)$$

Substitution yields:

$$9 * LO_2 = N * LO_1 + 300 \text{ MHz} - IF \quad (3)$$

Three alternatives have been considered:

1. IF = 20 MHz   N = 9 $\rightarrow LO_2 = LO_1 + 31.11$ GHz
2. IF = LO_2 N = 10 $\rightarrow LO_2 = LO_1 + 30$ MHz
3. IF = 300 MHz N = 9 $\rightarrow LO_2 = LO_1$

The first choice is driven by the idea that the 20 MHz IF can be fed directly into the HP8530, a common practise when using remote mixers. This choice has a few disadvantages. To provide the receiver with a stable reference signal for locking, a second (expensive) receiver module is required together with a directional coupler at the transmitter output. Besides that, 3 external sources are required: LO_1, LO_2 and F_{ref}.

The second solution is based on a configuration of an HP8511 frequency converter in combination with the HP8530, since this is part of the standard equipment of the CATR. The LO_2 source can be used for locking the receiver. An attractive aspect of this choice is that the triple frequency of LO_2 is

Figur 3: Complete system diagram.
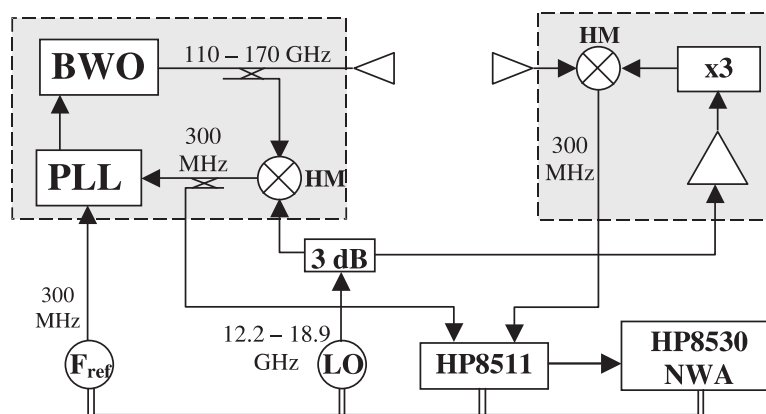
again a standard RF band, even for extensions up to 360 GHz (170 – 250 GHz, 250 – 360 GHz), which increases the availability of components. However, for the mixer operation it is not an optimal choice since the third harmonic of the IF is equal to the mixer-LO (= 3 * LO_2). This can give al kind of unwanted mixer products. And also in this case, 3 external sources are required.

In the last option, the IF is equal to the PLL reference frequency (300 MHz). Since LO_2 is equal to LO_1, only two external sources are needed and these can be controlled conveniently by the multiple source capability of the HP8530. A reference signal for locking the receiver and monitoring the TX-output can be obtained by a directional coupler in the line between harmonic mixer and PLL. This is the most attractive solution and has been implemented. The complete system is shown if figure 3.

Corrugated horns

The range feeds have been designed by the manufacturer of the ESTEC Compact Antenna Test Range, March Microwave. The manufacturing by means of electroforming has been done by Thomas Keating Ltd [7]. Several design iterations and a scaled test model at X-band have been made to match the design goals to the manufacturing limitations. The design goals could not be met over the full frequency range of 110 – 170 GHz. A much better performance has been achieved by covering this range with two antennas. In the last iterations, the horns have been optimised for equal E- and H-patterns, Cross-polar radiation in an area up to 12° from boresight (illumination of CATR reflectors) and Return Loss. Figure 4 shows a picture of the manufactured horns.

Figure 4: Corrugated Range antennas
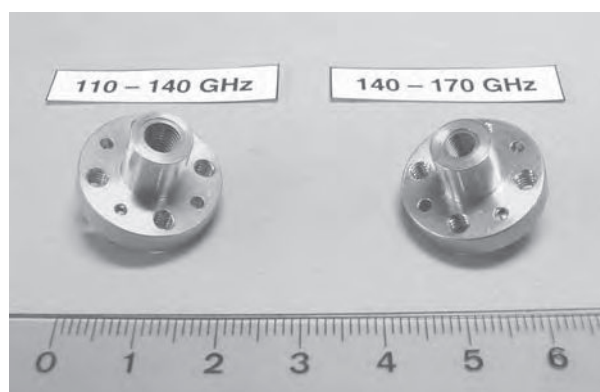
Some characteristic design numbers of the horns are:

Half cone angle:	10°
Corrugations:	13
Aperture diameter:	4.6 mm (110 – 140 GHz)
Directivity:	13 – 15 dBi
HPBW:	36°
X-polar:	< –40 dB for θ < 12°
Return loss:	< –25 dB
Waveguide:	WR06

Test data of the horns are not available yet.

Test results

At the moment of writing, the Factory Acceptance Tests have just been finalized. These tests were limited to the Transmit and Receive module of the system, the grey blocks in figure 3. The system integration with the HP8530 and HP8511 will be done on site at a later stage.

Figure 5 shows that maximum transmit output power is well above 10 dBm over the whole frequency range.
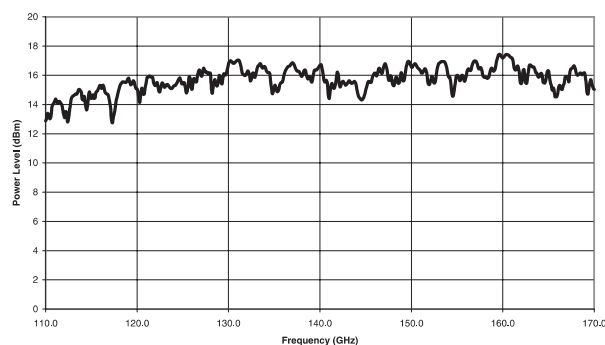
Figure 5: Maximum transmit output power of BWO-Tx module

The frequency spectrum at the 300 MHz IF reference channel of the TX module at the upper band edge of 170 GHz (see figure 6) shows that the spurious spectral components are below –60 dBc. The spectra at 110 and 140 GHz are similar.

Figure 7 shows the conversion loss of the Rx-module. The 15 – 20 dB assumption in the power budget of the introduction proves to be realistic, apart from the spikes. Since the results are fresh, there is no explanation yet for this spiky characteristic.
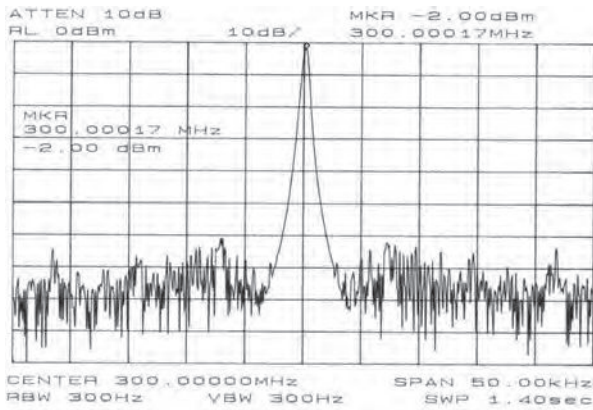
Figure 6: IF frequency spectrum of Tx-reference output for RF = 170 GHz.

Finally, in figure 8, the sensitivity of the receive module is shown.

These Factory Acceptance Test results show that the requirements for Transmit Power and Dynamic Range are achieved. Other intended features, like the compatibility with the HP8530 Network Analyser and the sweep capacity have to be proven during a Site Acceptance Test at a later stage. After that, the performance of the whole Compact Antenna Test Range, i.e. the Quiet Zone amplitude and phase ripple, has to be tested. But the realized equipment is a powerful and promising starting point for a Compact Antenna Test Range, capable of measuring at mm-wave frequencies with the same functionalities and error correction techniques as at lower frequencies.

Conclusions

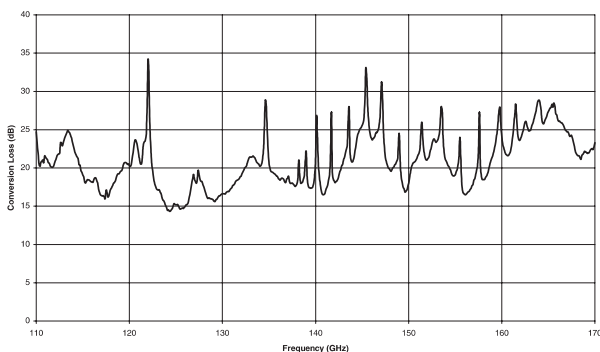The realized equipment for measuring antennas in the ESTEC Compact Antenna Test Range at mm-wave frequencies has unsurpassed performance in terms of band coverage, tunability and Dynamic Range. The concept is very attractive due to its compatibility with the widely used HP8530 Network Analyser. Another attractive point is the coherent measurement capability that enables the use of correction techniques like time gating (based on frequency to time conversion) and AAPC.

References

[1] D. Lamarre, J. Langen, C.-C. Lin, L. Marchand, P. de Maagt, T. Narhi, « Technological Needs for European Space Agency's Microwave Limb Sounders", *8th International Conference on Terahertz Electronics, 28-29 sept. 2000, Darmstadt, Germany*

[2] R. Zimmermann, "Millimeter and Sub-millimeter Wave Sources", P*roceedings of the 20th ESTEC Antenna Workshop on Millimetre Wave Antenna Technology and Antenna Measurement*, WPP-128, 18-20 June 1997, ESTEC, Noordwijk, The Netherlands, pp. 297-302.

[3] http://olesonmicrowave.com/index.html

[4] http://www.elva-1.spb.ru/

[5] http://www.farran.com

[6] J. Säily, J. Mallat, A.V. Räiisänen, "Using a Phase-Locked Backward-Wave Oscillator (BWO) to Extend the Dynamic Range of a Vector Network Analyser at Submillemetre Wavelengths", *Conference Proceedings of 31st European Microwave Conference*, London, 25 September 2001, Vol. 1, pp. 57 - 60

[7] http://www.terahertz.co.uk

Figure 7: Conversion Loss of Receive Module.

Figure 8: Sensitivity of Receive module at 140 GHz.
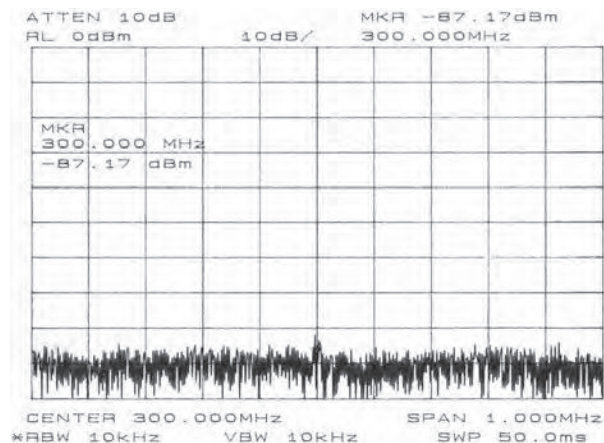
Authors

M.H.A. Paquay
ESA-ESTEC
P.O. Box 299
NL-2200 AG Noordwijk
The Netherlands
Email: maurice.paquay@esa.int

D.R. Vizard
Farran Technology Ltd
Ballincollig, Cork, Ireland.
Email: sales@farran.com

D. Korneev
ELVA-1 Millimeter Wave Division
DOK Ltd, Nevsky 74, 23N
St. Petersburg, Russia
Email: Korneev@exch.nnz.spb.su
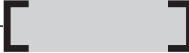
P. Ivanov
ELVA-1 Millimeter Wave Division
DOK Ltd, Nevsky 74, 23N
St. Petersburg, Russia
Email: Korneev@exch.nnz.spb.su

V.J. Vokurka
March Microwave Systems B.V.
De Huufkes 20
NL 5674 TM Nuenen
The Netherlands

Fasoren, een reactie op een reactie

P. van der Wurf

Uit de reactie van de heer Gestman Gerardts in nr. 1 (2002) van het NERG-tijdschrift blijkt dat sommige van mijn ideeën niet helemaal goed zijn overgekomen. Ik heb beslist niet - zoals Gerstman Gerardts stelt - stroom als een complexe e-macht willen weergeven. Mijn complexe e-macht is geen stroom, maar de fasor van een stroom, die gegevens herbergt over de amplitude en de fase. Anderen noemen dat de "complexe amplitude". Met de fasor kun je rekenen, zoals je ook met de amplitude of met de fase van de stroom kunt rekenen.

De fasor is zeker niet "een stroom of spanning waaruit de frequentie verdreven is", om de woorden van Gestman Gerardts te gebruiken.

Omdat de modulus en de fasehoek van de fasor beïnvloed kunnen worden door frequentie-afhankelijke netwerkelementen en omdat de mate van beïnvloeding mede bepaald wordt door de (vaste) frequentie van de stroom, is de fasor frequentie-afhankelijk. Deze frequentie-afhankelijkheid wordt teruggevonden in de uitdrukking voor de impedantie, die ontstaat uit het quotiënt van twee fasoren. (Zie de uitdrukkingen voor de stroomfasor bij spoel en condensator bij de formules (7) en (8) van mijn artikel.)

Omdat impedanties frequentie-afhankelijk zijn, vind ik het logisch om van impedantie-functies te spreken.

Large Space-Borne Antennas as a Tool For Studying the Universe at an Ultimate Angular Resolution

Kees van 't Klooster, Leonid Gurvits

Introduction

There are ongoing efforts to create new ground-based radio telescopes with a square kilo-meter receiving area in the not so far future [1]. It is a given physical fact, that the finite size of the Earth limits resolution capability in radio astronomical observations.

The first step on the way forward to exceed the resolution as imposed by the Earth limit in the radio domain is the use of space-based radio telescopes and to observe in an interferometric mode (Very Long Baseline Interferometry = VLBI) in conjunction with the ground-based radio telescopes.

The possibility of increased resolution capability in radio astronomy interferometric observations has been clearly shown recently with an inclusion of the space-based element in the VLBI-network. Several missions were proposed in Europe, the USA and the USSR in the 70's and 80's [3]. A Japanese satellite HALCA demonstrated this fact. It was launched in February 1997 and led to the VSOP program [2]. The launch of HALCA marked the brightest event in the history of Space-VLBI (SVLBI). Together with the terrestrial network it created the VSOP mission.

The technical feasibility of SVLBI was demonstrated by observations conducted with the communication satellite TDRSE in 1986 [11].
From the late-1970s through the early 1990s, at least four different dedicated space VLBI missions have been considered seriously. QUASAT [5] and the International VLBI Satellite [6,7] were proposed missions that did not receive final approval. HALCA (earlier VSOP [8,9]) is mentioned above and presented in this workshop [2] and is led by the Institute of Space and Astronautical Science in Japan. RadioAstron is a mission, led by the Astro Space Center of the P.N.Lebedev Physical Institute in Russia [4,10,36,37].

VSOP and RadioAstron are similar in character and in system sensitivity, with frequency coverage up to 22 GHz, 10-mclass radio telescopes with system temperatures near 100 K and data-acquisition rates of 128 Megabit/s. As described in [2], the 22 GHz channel in the VSOP mission experienced some problems after launch. The most important difference between the two missions is that RadioAstron is planned to have an apogee height of 80000km, providing baseline lengths of up to seven Earth diameters, while VSOP has an apogee height of 22000km, providing baseline lengths up to about 2.5 Earth diameters. These missions are sometimes referred to as first generation SVLBI missions.

The next generation SVLBI mission

Major characteristics for a next SVLBI mission, which will distinguish them from their predecessors , are:

1. A decreased system temperatures of the telescopes;
2. An increased data rate of the signal recorded;
3. An increased collecting area of each VLBI telescope,

Of these three main characteristics for a next SVLBI-mission, the latter seems to be of paramount importance and is of course of interest for the audience in this workshop.

- The first item is being actively investigated, with the goal of reaching a system temperature T_{sys} of about 10 to 20K for most operational frequencies in the ARISE mission, under consideration in USA [12,14,15].
  This development is matched by similar target

values for ground-based radio telescopes. However, further improvement of VLBI sensitivity due to decrease of T_{sys} is becoming asymptotically difficult as the values of system temperature reach single digits in Kelvin. Also other application scenarios are found, where such improvement in T_{sys} is of interest, like in other radio-astronomy (radiometric) type of missions (Planck for instance) and so such efforts are ongoing.

- The second item is also being actively pursued. It is foreseen that a data rate of 1 Gbit/s will become available in a few years [16,17]. Apart from the fact, that ITU regulates available bandwidths, there is also a practical limit on the width of the signal: the bandwidth must not exceed a reasonable fraction of the sky frequency of the observations. In addition, a major drawback of this venue for sensitivity improvement is its irrelevance to spectral line VLBI.

- The remaining third item, the increase of the collecting area of each element of the VLBI array, remains the only option that is practically unlimited and equally efficient for both continuum and spectral line VLBI observations.

As discussed in [2], possibilities for a follow-up mission (VSOP-2) are investigated. There is the ARISE initiative [12,14,15], relying on an inflatable antenna with a size of the 25-m diameter. An inflatable antenna was considered for QUASAT [5,23,30] and studied for land-mobile applications with demonstration models [24].

If steps to the higher frequency bands are implemented, it implies, that the reflector antenna must have an rms accuracy of circa 0.2 mm, in order to be operational at wavelengths as short as 3 mm (86 GHz), a target requirement for the ARISE mission. Error correction techniques, using self-focussing approaches were proposed, but then the calibration aspects might be displaced to the calibration of the feed-arrays to be used. NRAO elaborated such a technique [25], but obviously much more work is needed.

There is clearly the interest to explore the larger space-borne antenna as SVLBI element

Use of the international space station (ISS) for construction of a large antenna

Traditionally, SVLBI is considered as a single launch mission with no in-orbit assembly operations. Three possible technologies have been investigated for forming the reflecting surface in the antenna, namely: inflatable, mesh or solid material structure. All three options require in-orbit deployment of the antenna and associated with the launcher capability (fairing size), which is a limitation for each type of technology in terms of stowage volume and resulting antenna diameter.

Roughly the largest diameter possible for the stowage volume fixed is achieved with an inflatable technology, followed by the mesh technology with straight or foldable ribs. The solid panel approach is less economic in terms of stowing within a given volume.

But in particular the requirements for the larger diameter and at the same moment the requirement of a better surface accuracy as needed for the higher frequency band are contradictory and for this intuitively the preferred technology is the one with solid panels. The RadioAstron mission relies on a solid panel type of antenna, however the stowage during launch and subsequent deployment scenario are factors, which have serious impact on the achievable surface accuracy [4,10,36,37]. Once deployed in orbit with the desired shape, the antenna construction has a very long lifetime.

Here we consider an approach, which may be beneficial for the demand of high surface accuracy as well as for a realization of a larger diameter. The concept for a next SVLBI mission is discussed with a 25-30 meter class radio telescope, which is to be assembled in space, with – in outline format - dedicated attention to antenna problems .

The International Space Station (ISS), a permanent multi-purpose orbital manned facility, is considered as a base for the telescope assembly. There are plans to use the ISS as a place with infra-structure assembling and/or servicing freeflying scientific missions (X-ray Evolving Universe Spectroscopy or XEUS [19,20,21]). The X-ray lens as considered for XEUS has also sub-millimeter focusing capability and as such a function in the sub-mm or IR-domain (with reduced efficiency, but better resolution than Herschel) could be of interest.

It seems logical to consider ISS as a building place for a large space-based radio telescope, which can then be sent into a dedicated orbit, away from the ISS. Servicing would be also possible eventually, after docking of the spacecraft with this radio telescope.

A mission using a multiple launch and in orbit assembly is an alternative to a single launch concept with limited cargo capability. Such an approach makes it possible to accommodate an antenna of considerably larger mass, and therefore larger diameter and better surface accuracy. The multiple launch concept could be combined with all three antenna designs above (inflatable, mesh and solid panel technology). However, obvious advantages of a multiple launch scheme are clearly for a solid petal antenna especially as such configuration is of interest to go to higher frequency. Since the assembly is likely to require manned operations, it is logical to consider the International Space Station (ISS) as the base for such a next SVLBI mission. In general, it is imperative for the ISS to become an assembling facility for future large orbital or interplanetary missions, as assumed already for XEUS [19,20,21].

The spacecraft module with the large SVLBI-antenna assembled should have the ability to function in a free-flying regime as well as docked to the ISS. It can reach the ISS in autonomous flight or be delivered to the ISS by a Space Shuttle or other transport spacecraft. In the former case, the module must be equipped with a full set of systems

for autonomous flight, rendezvous, proximity operations and docking. Most of these could be utilized for autonomous flight after assembling the radio telescope. The set of antenna reflector elements (panels) could be delivered to the ISS by a Space Shuttle or by another transport vehicle involved in the ISS logistics.

The main requirements for the module spacecraft of for a next SVLBI mission and the overall mission operational issues are quite similar to those of several other applications, like astrophysical and Earth science missions, that do not need to be permanently located at the station. A very high level of commonality in major mission requirements could be pursued and reached between the SVLBI-concept described here and the XEUS mission [19,20,21].

The assembly of the radio telescope would be carried out in the docked position (fig.1). It would utilize the available robotic mechanisms on the ISS, like the European Robotic Arm, ERA, and the Canadian Space Robotic Mechanisms. It would require some extra-vehicular activity by the station crew. A possible scenario for a next SVLBI radio observatory assembled in Space is described in [19]. Two important aspects in this scenario are underlined:

1. The SVLBI radio telescope occupies one of the ISS docking ports for a very limited time (approximately one month - tbc) and leaves the

Figure 1: Conceptual illustration showing a large 25 meter diameter antenna during assembly on ISS.
Courtesy- EADS Les Mureaux
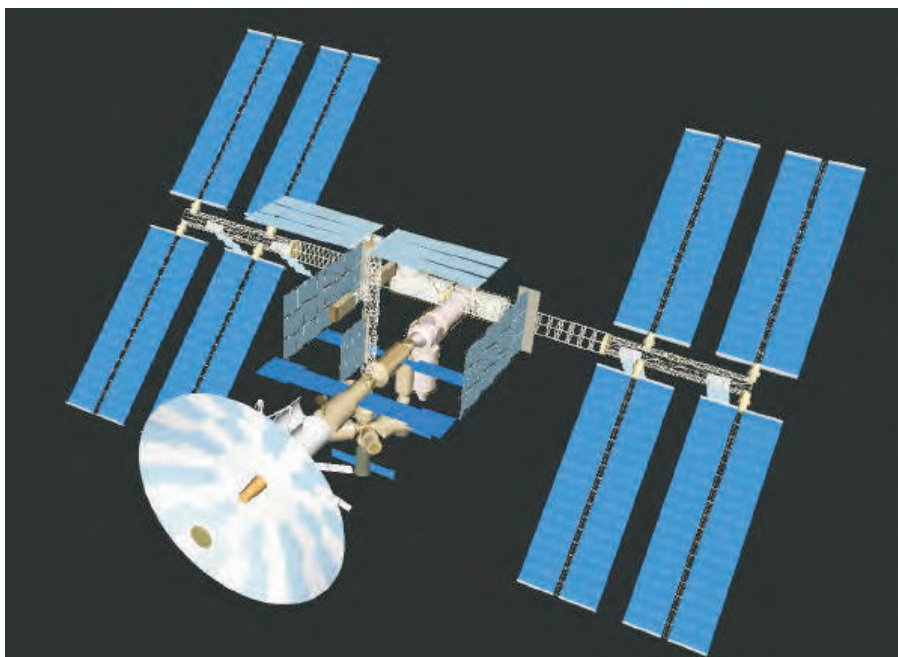
ISS low orbit after completion of assembly and test operations;

2. The in-orbit checkout of the telescope starts while the SVLBI spacecraft is docked at the ISS. The latter provides the opportunity to fix most possible problems – if any - with the SVLBI-2 spacecraft before it goes into autonomous flight.

Multiple launch and in-orbit assembly of a next SVLBI-mission could bring technical, budgetary and logistical advantages over traditional single-launch in-orbit deployment schemes. The in-orbit assembly concept should therefore be explored at the earliest stages of the next SVLBI-mission design studies. Such a scheme could also bring additional benefits (in the form of decrease in per-mission cost) by sharing substantial parts of its overall cost with other ISS applications.

This idea to use International Space Station has been preliminary investigated in the sense of infrastructure and mechanical by EADS, with exploitation of transfer logistics (ATV) and robotics available on ISS for the construction of a large radio telescope. However, background information and further suggestions for a large space based radio telescope need to be investigated in more detail. Certain antenna configurations are more suitable in ergonomic sense (for the robotics available) for assembly at ISS. This paper attempts to indicate this by some further background information and some suggestions, which could be discussed further.

Two indicative directions to realise a large radio telescope, based on available technologies, are put forward for further exploration. Obviously the scenario invites for alternatives. A study of a realisation of a large radio telescope in space, considering International Space Station as a shipyard to construct the large radio telescope, would require combined efforts of all disciplines (radio-physical, mechanical, robotics, ergonomics, transportation). Different technologies could then be revisited, also imposing constraints and inputs on antenna design capabilities. The antenna reflector assembly would require a backing structure with a main reflector assembly, a sub-reflector supported somehow by some structure to support the latter. No decision is made at all for a particular scenario and an off-set (like the Green Bank radio telescope [26]) or a symmetrical parabolic or shaped or even deviating shape can be considered. Once more the required

trade-offs in close cooperation with all disciplines involved are emphasised.

Today it is common practice in the realisation of ground-based radio telescopes to have the main reflector built up out of separate reflector panels [22], even at sub-millimeter wavelength. A suitable backing structure and an optimisation of the number of panels would permit for our SVLBI-mission to realise a main reflector assembly. Also the offset scenario as used for [26] would permit to have identical panels along partial rings with the focus of the describing parabola for the offset geometry as center.

Two potential scenarios for the backing structure could be imagined:

1. Use of a truss, which still may have some limited foldability if needed for easier transfer in a cargo ship or which can be consisting out of sub-segment trusses.
2. Use of a radial rib structure as considered already some decades ago for large deployable antennas [27,28].

There have been studies in the past for deployable truss-type of antenna support structures . The 6 meter Travers antenna and the KRT-10 antenna belong to this category [33,34]. Also a truss-type structure was tested in space in early 80, with extra-vehicular activity performed by the French astronaut. Fig. 2 shows the TRAVERS antenna, which has been used in a L-S band SAR on the Priroda platform (connected to MIR). It was considered as an element of an array of three reflector

Figure 2: TRAVERS antenna, used for L-S band SAR on Priroda (MIR), courtesy OKB-MEI
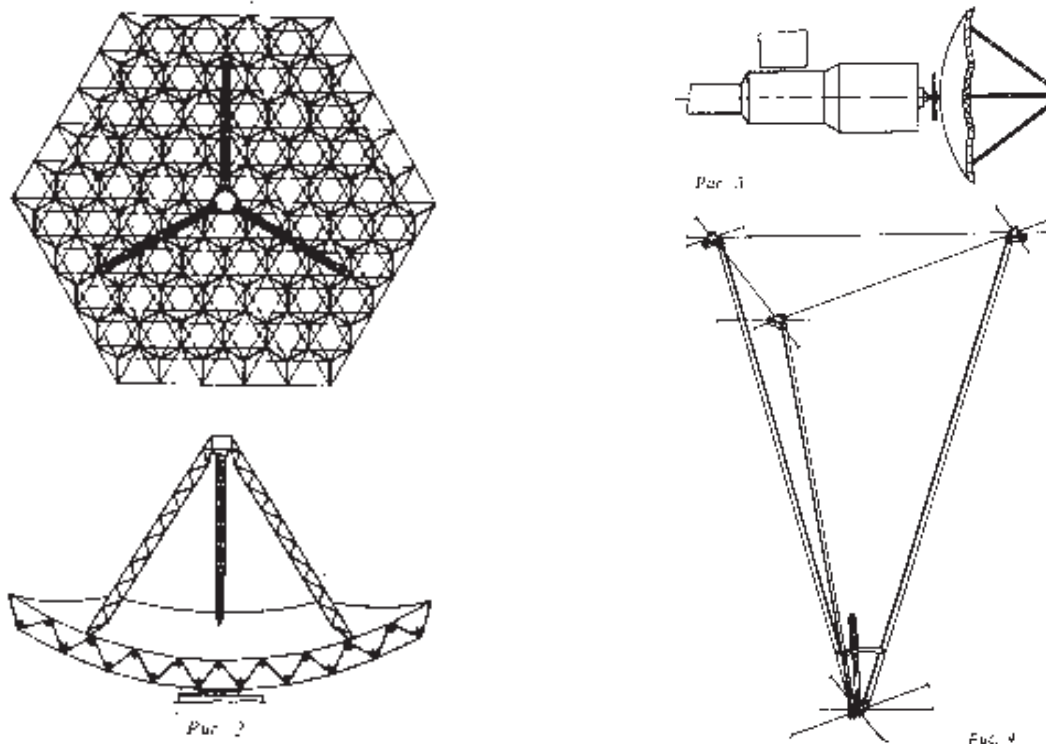
Figure 3: Picture KRT 10 [33], mesh carried on ropes. In the same reference anothertruss design is discussed.

antennas for a SAR on-board the ALMAZ II space-craft.

Already in 1979 a 10-meter radio telescope has been flown on the space-station at that time (note some synergy with the proposed concept here), the Sal-joet 6. Two concepts have been investigated in that interesting time, based on a space 'truss', suppor-ting a mesh reflector antenna. One concept relied on the space truss constructed out of rods only (with where needed mechanisms to fold and stretch) [34], where as the other concept relied on replacing part of the rods by wires and in this way the 10-meter KRT -10 antenna was realised [33].
This KRT-10 antenna had thus a space truss, where the upper and lower surface was provided by a wire configuration. The mass was at that time about 300 kilogram, with 60 kilogram for the reflector.
Fig.3 shows the stowed configuration of the KRT -10 reflector with its three struts supporting a feed container (note: these struts are about 6 meter in length). Fig.3 shows also the reflector configuration and the schematic drawing of the antenna attached to Saljoet 6 as well as the system of utilisation of wires and rods. Russian for mesh is 'setka' or net. The Russian kosmonaut was almost catched in the net, when he had to release the antenna before

ending his mission. Another antenna configuration based on a space-truss with rods was investigated (5-meter antenna model realised and electrically tested). The 5-meter antenna weighed 43-kilogram [34] and electrical tests were carried out before any electrical test activity was realised for antennas as reported.

A similar type of antenna (fig.2) was used in a reflector based SAR and did show functionality with the SAR on Priroda, operating in L and S-band, but there were other problems with MIR to fully exploit the SAR instrument capability. Fig. 4 shows this antenna on MIR.
A thin mesh is carried on top of the space truss. The antenna is stowed, such, that deployment is done from the centre, which implies, that the last phase of the deployment is more critical. Then the struc-ture has to stretch the reflector mesh, while it is still deploying from the centre. The space truss was tested in the early 80's. The realisation of the mesh at that time was supported by various activities at the textile institute [35]. Anticipating the realisation of an accurate reflector antenna for Space VLBI: such a space-truss could provide a carrying struc-ture, not only for a mesh but also for an antenna with reflector-panels forming the main reflector, thus a potential functional technology for a realiza-

Figure 4: Antenna of the L – S band SAR on the Priroda platform on MIR (+).

tion of a large radio telescope antenna, suitable for shorter wavelengths.

Large deployable reflector antenna (georgian polytechnical institute, tbilisi)

In the early 80's other investigations resulted in models of deployable antennas with 30-m diameter. Such constructions were realised in a dedicated location near Tbilisi, specially equipped with facilities to explore various aspects, like zero gra-

vity, owned by the Georgian Polytechnical Institute. There was collaboration with the Moscow-based institute 'Kometa'. The Georgian Institute is specialised in deployable structures (also called: Large Transformable Structures). [28]. The interesting aspect is, that this type of deployable reflector antenna relies on a deployable pantograph, which, once deployed, still provides forces to stretch a reflector surface and a radial blade assembly at the end of the deployment phase. Different models have been realised and an annular deployable ring was flown on 'Progress-40' (called 'Krab').

Also the linear deployable mast was realised and currently flies on MIR (Sofora). The latter mast on MIR has been used as attachment location for the flight experiment with the large deployable antenna (7 meter diameter) with annular deployable pantograph to demonstrate another time the suitability of such structure for a large deployable antenna (see also related papers in this workshop [37]).

A 13-meter model was realised in co-operation with DASA (Dornier) In November 1997, two successful deployment demonstrations have been carried out in the special facility in Tbilisi. The figures on this and the next page show different moments during a deployment. The end result is a configuration, which is of interest: a deployable annular pantograph with a radial blade configuration. Such structure inherently provides an interesting frame-

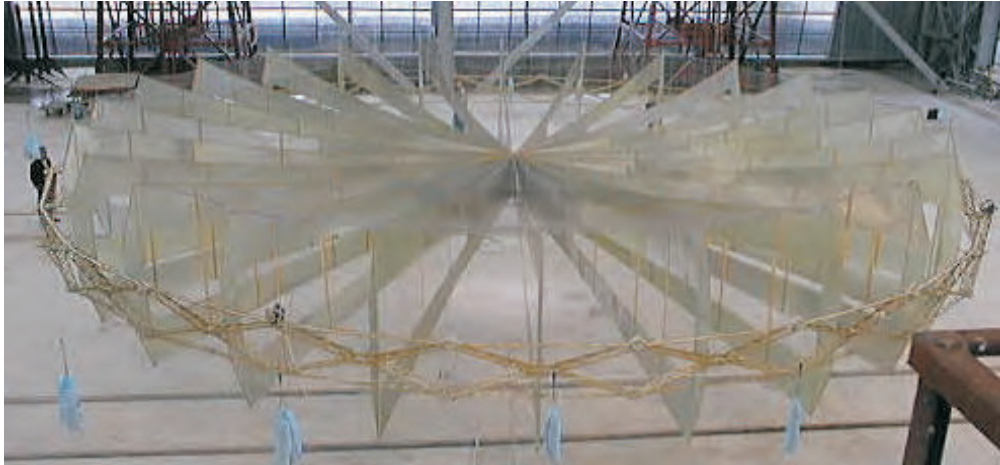Figure 5: Large Deployable Offset Reflector in Tbilisi GPI Facility.
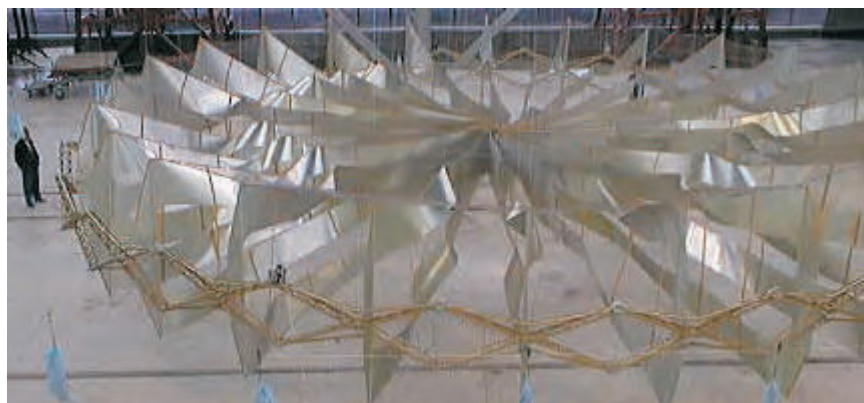
Figure 6: The interesting feature is that the radial ribs provide attachment capability with good accuracy in axial sense.

work, on top of which one could consider to attach some reflector assembly constructed out of thin reflecting panels. The configuration shows an annular pantograph with diagonal elements. Other pantograph concepts have been investigated as well and implemented in working models. The experiment on MIR found its origin here [37], see also [27].

SVLBI antenna to be assembled on the ISS

Especially a larger size reflector antenna is an object, for which potentially the use of the ISS is of interest. Radio astronomers are interested in a radio telescope with an 'as-large-as-possible' effective receiving area. In a previous part various deployable antenna concepts or related technologies were indicated, showing that such subject has a wide attention. In complement other large antenna designs (for Thuraya, Aces, Inmarsat, - See also other contributions in this workshop) have to be mentioned. The aspect of stowage during the launch and a deployment in space is nevertheless an factor of impact.

When now the ISS is used, the stowage and deployment aspect is no longer present. This is of high interest, in view of the absence of dedicated activities related to a guarantee with high reliability a very precise deployment in space after stowage in the launch vehicle. This is an important advantage of using the ISS. ("Sometimes mechanism-specialists indicate, that the best mechanism is 'no' mechanism"). An absence of deployment errors leads to a better surface error budget. The antenna, which will be assembled on the ISS, deserves further investigation, in which the absence of various

aspects related to deployment reliability should be explored in detail, with impact on the total accuracy.

The actual configuration as studied preliminary (fig. 1), was taken from the IVS study [6,7]. However, the application of such an antenna for different type of scientific observations may have an impact on the desired precise reflector shaping. An initially anticipated configuration might be a dual shaped reflector antenna, eventually even (partly) offset, but such decision depends on the total picture, including the ergonomics in assembling.

The interest in shorter wavelength bands implies that mesh as reflecting surface are not a priori preferred, especially when frequency bands well above 20 GHz are needed. Therefore solid surface panels (or approximating even foil type of structure) or even a subdivision of the reflector surface into a set of panels has to be looked at. Such an approach may include a panel subdivision comparable to scenarios as applied in ground station antennas, like for instance the ESA 35meter antenna for Deep Space applications [39].

The difference with ground-station antenna is clearly the massive backing structure in the latter, needed to provide the similar reflector shape under various loading conditions (gravity, wind, thermal, etc.) Panel solutions are explored for the Radio Astron antenna and indeed panel measurements during thermal vacuum conditions have demonstrated sufficient surface accuracy at panel level to move to high frequency bands. Such a type of panel technology is therefore also of interest [36].

A very interesting panel technology is today realised as a technological spin-off using the manufacturing techniques developed for the X-ray satellite XMM [22,31]. As described in [22], it is currently a very attractive way of realizing antenna reflector panels, using electroforming as replica technique. It has high potential for sub-mm wave antennas like for instance the ALMA radio telescope. For an eventual realization of a large reflector, consisting out of panels it becomes interesting again, although the approach might be quite different as considered for a terrestrial sub-mm wave radio telescope. But such a panel technology is of high interest, especially for a realisation of a larger size reflector surface, to be assembled with the aid of the infrastructure available on the International Space Station ISS.

At this stage it is of interest to explore as much as possible consolidated technologies as made available already from earlier studies and to combine partial solutions and indicate ways forward.

Other applications may also benefit from such approach (microwave power transfer, solar power generator, antennas for remote sensing applications, telecommunications at high frequencies).

Roadmap for a way forward for a large 25 to 30 meter radio telescope

The suggestions given are based on available technologies or linked to it.

1   **Investigation of backing structure as designed already by the Georgian Polytechnical Institute.**

This type of structure as shown in fig 5 and 6, provides, with the annular pantograph as relatively reliable azimuthal structure, together with the radial ribs with a relatively good axial stiffness, a promising backing structure, on which - using ISS and robotics - a panel layout could possibly be realised. A panel-subdivision could be very much comparable to a panel sub-division used for instance the ground-station antenna [39] planned for Rosetta (35-m diameter). Panels with a size of about 2.5 a 3 m by 2.5 a 3 meter are considered for the 35-m ground station. Detailed panel design, based on nickel-electroformed panels is a potential consideration for ground-station antennas (as well as for radio telescopes like expected in the ALMA project). Electroformed nickel panels with side edges for stability at panel level might be considered potentially for this space based radio tele-

scope. As indicated in [22] larger panel sizes were investigated as well, but further work is needed to control the parameter setting for space conditions. The accuracy setting as realised today [22] of below 10 µ (rms) surface error (compliant with ALMA requirements) is not needed

either for the large radio telescope. Electroformed panel-technology has been explored before [38].

If sidewall ribs are applied for the nickel sheets, to provide additional axial rigidity, an assessment shall be made, related to the optimum panel sizing and the suitable backing structure (i.e. nr of ribs) as well as the use in connection with robotics. Eventually the magnetic aspect of Nickel may be not desired in certain applications (non-magnetic materials sometimes not desired, impact of magnetic moment and associated torque together with fine-pointing aspects), but on the other hand, magnetic aspects may assist to control the panel gaps. This all requires further investigation. Use of 90 degrees ribs connected to the panels shall be considered in relation to the associated stowage of a pile of such panels during transport and the necessary robotics on the ISS to deploy.

2   **Utilisation of a space-truss structure, on which a panel lay-up can be realised.**

Again panel subdivision can be possible, comparable to a subdivision as used for ground station antennas, but more detailed study is needed. Hexagonal subdivision might be a more natural way to explore the nodal subdivision of the space truss. Hexagonal panel re-distribution has been suggested earlier, for instance in early US studies. (See also ESA Workshop 1984, SP-225, J. Hedgepeth – ASTRO).

Conclusion

Radio astronomers exploiting VLBI-techniques have a need for space-borne radio telescopes in order to exceed the angular resolutions as imposed by the finite Earth diameter. The first generation VLBI mission VSOP has clearly demonstrated the potential for high resolution Space-VLBI. The next steps are investigated. A large effective receiving area (stabile with wide-band receiving capability) is an imperative for progress in radio astronomical studies . A suggestion is put forward to use the ISS as a facility, where a larger radio telescope can be assembled, before it is put in its desired scientific orbit for observations. As described, this concept is based on the available technologies. Today the

state of these technologies is even further advanced, and in part well known to the audience, but no exhaustive referencing has been done here. We note a considerable level of synergy between this concept and the technologies exploited on-board the ISS (e.g. robotic arms, in -orbit assembly operations). Further study can detail these aspects.

References

[1] http://www.astron.nl/, follow indication SKA

[2] Hirabayashi, H. "Experiences with the HALCA Space VLBI Satellite and Plans for the Future", 25th ESA Antenna Workshop, Noordwijk September 2002.

[3] Ulvestad J.S., Gurvits L.I., Linfield R.P., 1997, in High Sensitivity Radio Astronomy, eds. N.Jackson and R.J.Davis, Cambridge Univ. Press, 252

[4] Kardashev N.S. & Slysh V.I. 1988, in The Impact of VLBI on Astrophysics and Geophysics, IAU Symposium No. 129, Eds. M. J. Reid and J. M. Moran, Dordrecht: Kluwer Academic Publishers, p. 433

[5] Schilizzi R.T. 1988, in 'The Impact of VLBI on Astrophysics and Geophysics', Proc.of the IAU Symp. No. 129, eds. M. J. Reid and J. M. Moran, Kluwer, 441

[6] Pilbratt G. 1991, in 'Radio Interferometry: Theory, Techniques, and Applications}, eds. T. J. Cornwell and R. A. Perley, Astron. Soc. Pacific Conf. Series, 19, 102

[7] van 't Klooster, C.G.M. 'Space VLBI, A Proposed Antenna Configuration for the Radio Astronomy Satellite IVS', Proc. 2nd Int. Conf. Electromagnetics in Aerospace Applications', ICEAA, Sept 1991, Torino.

[8] Hirosawa H. & Hirabayashi H. 1995a, IEEE AES Systems Magazine, June 1995, p. 17.

[9] Hirosawa H.& Hirabayashi H. 1995b, 46th International Astronautical Congress, Paper IAF-95-Q.2.01.

[10] http://www.asc.rssi.ru/radioastron/Description/intro_eng.htm

[11] Levy G.S. , Linfield, R.P. Ulvestad, J.S. et al. 1986, Science, 234, 187

[12] Ulvestad, J.S. and Linfield, R.P. 1998, IAU Colloquium 164, ASP Conf. Series 144, 397

[13] http://www.astron.nl/documents/conf/science_index.htm

[14] http://arise.jpl.nasa.gov/

[15] http://us-space-vlbi.jpl.nasa.gov/

[16] Whitney, A.R. 1999, New Astronomy Review, 43, 527

[17] Cannon, W.H. 2000, Advances in Space Research, 26, No. 4, 747

[18] Gurvits, L.I. 2000, Advances in Space Research, 26, No. 4, 739

[19] Bavdaz, M., Peacock, A., Parmar, A. et al. 1999, in ' Utilisation of the ISS, ed. A.Wilson, ESA SP433, 621.

[20] ESA Bulletin May 2002 (ESA Estec Noordwijk) http://esapub.esrin.esa.it/bulletin/bullet110/parmar.pdf

[21] ESA Bulletin May 2002 (ESA Estec Noordwijk) http://esapub.esrin.esa.it/bulletin/bullet110/bavdaz.pdf

[22] G. Valsecchi, J.Eder, G.Grisoni, C.G.M. van 't Klooster, L. Fanchi, 'High Precision Nickel Electroformed Panel Technology for Sub Millimetre Radio Telescope Antennas', this 25th ESA Antenna Workshop.

[23] QUASAT, A Phase A Study, ESA contract CR(P)2914 and SCI(88)4, 1988, ESA (SCI(88)4 available still).

[24] Electrical Performance of a 10 Meter Inflatable Reflector for Land Mobile Communications, P.M. Besso, K. van 't Klooster, W. Rits, D. Savini, P. Tatalias, IEE, Int. Conference on Antennas and Propagation, York April, 1991.

[25] Self Calibration of Antenna Errors Using Focal Plane Arrays, P.J. Napier, T.J.Cornwell, 'Multifeed Systems for Radio Telescopes', ASP Conf Series Vol 75, 1995, Tucson, Arizona.

[26] http://www.gb.nrao.edu/GBT/

[27] G.G. Kinteraya, E.V. Medzmariashvili, L. Sh. Datashvili '5 - 30 Meter Deployable High Precision Light Weight Space Antenna Reflectors and the Ground-based Stand-test Complex for Assembling and Testing Large Deployable Space Structures', Keynote Paper Int. Conf. on Space Struct , Braunschweig, Nov.1998 (ESA sponsored).

[28] E.Medsmariashvili, 'Transformable Constructions for Space And Earth based Application (Russian)', Monograph, published by GPI, Tbilisi, 1995 (gpispace@access.sanet.ge)

[29] Space VLBI: Radio Astron and its Large Deployable Antenna. V. Babyshkin, In "Large Antennas in Radio 110, Noordwijk.

[30] K. van 't Klooster, W.Rits, E.Pagana, P.G.Mantica, M.C.Bernasconi, 'An Inflatable Parabolic Reflector Antenna: Its realisation and Electrical Predictions', ESA Journal 1990,Vol.14 (also Int. Conf Antennas, Riga, 1990).

[31] G.Valsecchi, C.Francini, R.Garcia Prieto, K.van 't Klooster, 'Nickel Sandwich Technology for High Precision Reflector Antennas', IEEE APS, Orlando 1999.

[32] H.Kellermeier, W.Schaefer, H.Vorbrugg, 'Offset Unfurlable Antenna Concepts' MBB (Now Astrium), ESA/Estec Workshop on Mechanical Technology for Antennas, June 1984, SP225.

[33] A.G.Sokolov, A.S.Gvamichava,, 'Decisions for the Engineering Construction of Space Based Radio Telescopes', (in Russian), 'Antennas', Volume 29, 1981,

[34] A.F.Bogomolov, N.V.Bykarev, G.N.Vachensjev, Yu.A.Kisanov, N.M.Feysulla, I.F.Sokolov. 'Deployable Antenna for Space Applications', (Russian), 'Antennas', Volume 29, 1981,

[35] Yu.A Kisanov, N.M. Feysulla, L.A.Kydrjavin, V.A.Savaryev, 'Materials for Reflecting Surface for Deployable Antennas for Space', (in Russian), 'Antennas', Volume 29, 1981,

[36] A.S.Gv amichava, A.N.Kotik, V.Babyshkin, V.Perminov, M.Bolotov, G.Mersch, H.van Oel, C.G.M. van 't Klooster, 'Accurate Surface Shape Measurements of 3.75 meter CFRP Antenna Panels for the Radio Astron Antenna Estec Workshop Antenna Technology, 21-23 Nov. Noordwijk, 1995.

[37] http://egs.cosmos.ru/freport.htm

[38] V.S.Poljak, E.Ya. Bervalds, 'Precision Constructions for Mirros for Radiotelescopes' Acad. Sci Latvia, ISBN 57966-0164-4 Published in Riga, 1990, page 166.

[39] R.Martin, D.Atkins, 'First ESA Deep Space Antenna in New Norcia West Australia', this workshop proceedings.

Authors

Kees van 't Klooster,
ESA Estec
Keplerlaan 1, P.O.Box 299, 2200 AG Noordwijk, The Netherlands
Email: kvtkloos@estec.esa.nl

Leonid Gurvits
Joint Institute for VLBI in Europe (JIVE)
P.O.Box 2, 7990 AA, Dwingeloo, The Netherlands
Email: lgurvits@jive.nl

Vervolg van pagina 134

Omdat impedanties frequentie-afhankelijk zijn, vind ik het logisch om van impedantie-functies te spreken. We hebben het in de systeemtheorie immers ook over overdrachts*functies*. De notatie $Z(\omega)$ doet studenten eraan herinneren dat impedanties functies van de frequentie zijn en dat helpt misschien voorkomen dat ze schrijven:

u(t) = Z. i(t) en dergelijke onzin.

Ik wou overigens dat ik als docent had beschikt over de twee didactische handigheden, die Gestman Gerardts noemt in zijn reactie en die op een eenvoudige manier aannemelijk maken dat een factor j een fasedraaiing van 90 graden geeft en dat de formule van Euler niet zo vreemd is als het lijkt. Conclusie? Docenten en oud-docenten moeten veel meer publiceren over hun ervaringen met de didactiek van de theoretische elektrotechniek. Een nieuwe functie voor het NERG-tijdschrift?

P. van der Wurf

Synthesis of Conformal and Miniature Antennas

Hubregt J. Visser, Jan Jonkergouw, Jos C.J.M. Warnier

Introduction

The continuing miniaturisation of handheld tele-communication equipment has led to the situation where the antenna has become the volume-defining component of today's portable and wearable products. A further miniaturisation requires first of all the antenna to be miniaturised even beyond today's standards. As a consequence of this miniaturisation, the antenna can no longer be regarded as a stand-alone component. This means that antennas need to be designed, incorporating effects of finite ground planes and substrates, dielectric covering and metallic and dielectric objects in the immediate neighbourhood of the antenna.

An example of a miniature antenna is shown in fig. 1. The antenna consist of a meandered conducting strip above a ground plane, short circuited at one end and excited by a probe through the finite ground plane. The dimensions of this antenna are $0.043\lambda_0$ x $0.043\lambda_0$ x $0.00583\lambda_0$, where λ_0 is the free-space wavelength.

The antenna shown in figure 1 has been designed by a (manual) iterative use of ANSOFT's HFSS© full wave 3D electromagnetic solver. Although full wave solvers have become very fast over the last couple of years, the design method as used for this antenna is very time consuming. Due to space restrictions and future need for enhanced bandwidth, it is expected that future antennas also need to be conformal (curved), thereby even further increasing design time. So, design time is expected to increase while at the same time a sharp decrease in time –to-market can be observed. The need thus exists for a very fast software tool for generating a starting configuration. As a pay-off for speed, the accuracy of the underlying model for this tool can be relaxed a bit, since the full wave solver will be used for fine-tuning the initial design. The purpose of the fast tool is to speed up the beginning of the design process.

As a first step in the development of such a tool, we have chosen the short circuited strip antenna on an infinite ground plane as basic radiator and investigated the feasibility of using analytical models and global optimisers to generate starting configurations for full wave solvers. In the remainder the first results will be presented.

Short circuited strip radiator

The Short Circuited Strip (SCR) radiator can be regarded as originating from the PIFA [1] or quarter wave microstrip patch radiator [2], see

Fig. 1: Miniature planar antenna and simulation results for the return loss.

---
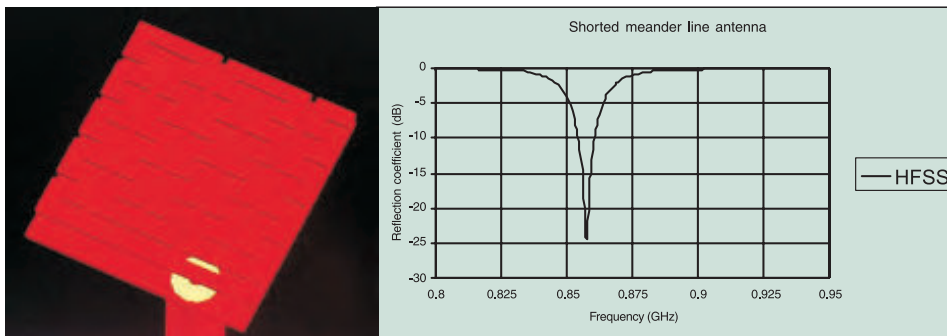
1   Jan Jonkergouw is currently with Philips Medical Systems Nederland B.V., PO Box 10000, 5680 DA Best, The Netherlands, E-mail: jan.jonkergouw@philips.com
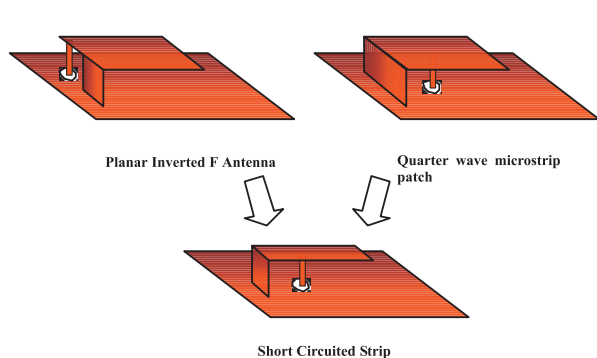
Planar Inverted F Antenna

Quarter wave microstrip patch

Short Circuited Strip

Fig.2: Short Circuited Strip radiator originating from PIFA and quarter wave microstrip patch

fig. 2. One of its main features is the relatively narrow width of the strip.

Although the strip can be positioned on a dielectric substrate, we have specifically chosen for a self-supporting structure in air, thus enabling ease of production and reducing costs.

A nice feature of the SCS is that an equivalent RC-network can be drawn by inspection, see fig. 3. From this network it is also evident that the length of the strip can be reduced (further than a quarter of a wavelength), by intervening in the right-loop series inductance, capacitor or both. Fig. 3 shows two examples of SCS antennas, miniaturised this way. Fig. 1 shows an example where the means of miniaturisation have been exploited to the full. The analytical model for generating the starting structure for the full wave solver must be capable to handle these deviations from the basic SCS structure. Promising analysis methods therefore are the Transmission Line Method and – to a lesser degree - the Cavity Method in combination with the

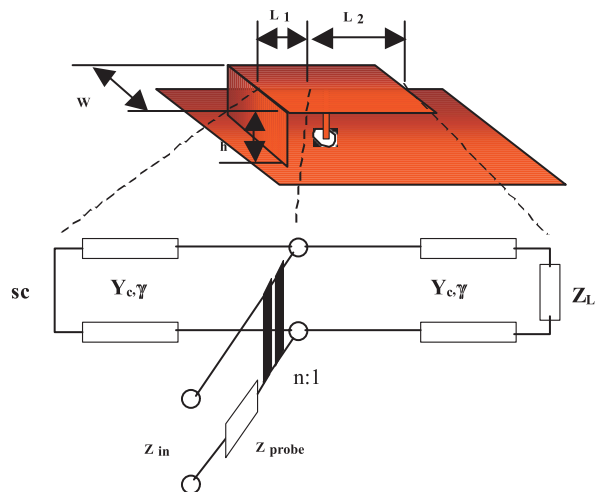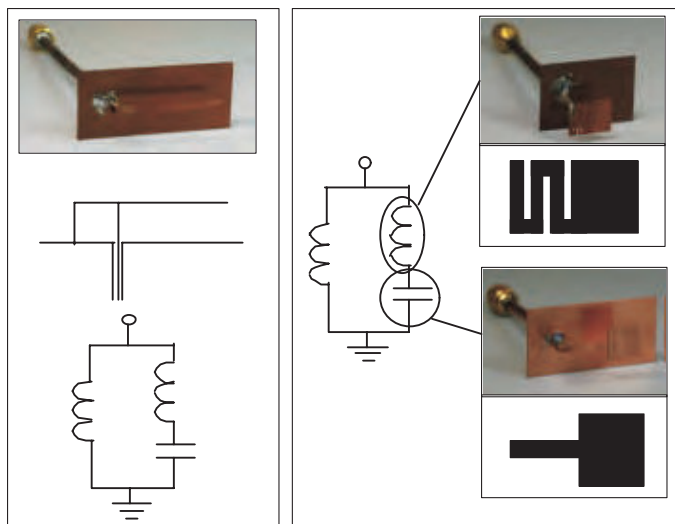Fig.3: SCS intuitive model and miniaturising deviations based on this model

Fig.4: Circuit representation of SCS radiator

Desegmentation Method [3]. The analysis method needs to be fast, where a reduction in accuracy will be allowed, since the fine-tuning will be performed with the full wave solver.

Microstrip line model for planar SCS-radiator

The Transmission Line Model follows from the Improved Transmission Line Model for rectangular microstrip antennas from Van de Capelle [4]. The probe is modelled according to [5, 6]. Adapting the two-slot model [4], we can simplify the circuit representation by short-circuiting one of the self-admittances representing the open-end terminations and omitting all voltage–dependent current sources, representing the mutual coupling between the slots. The circuit representation for the SCS radiator then reduces to the one shown in fig. 4.

The fringe fields are taken into account by lengthening the transmission line with Δl [4, 7]:

$$\Delta l = h\, \xi_1 \xi_3 \xi_5 / \xi_4 \tag{1}$$

where

$$\xi_1 = 0.434907 \frac{1 + 0.26\,(W/h)^{0.8544} + 0.236}{1 - 0.189\,(W/h)^{0.8544} + 0.87} \tag{2}$$

$$\xi_2 = 1 + \frac{(W/h)^{0.371}}{3.358} \tag{3}$$

$$\xi_3 = 1 + 0.5274 \arctan\left\{0.084\,(W/h)^{1.9413/\xi_2}\right\} \tag{4}$$

$$\xi_4 = 1 + 0.0377 \arctan\left\{0.067\,(W/h)^{1.456}\right\} \tag{6}$$

$$\xi_5 = 1 - 0.218 \exp(-7.5W/h) \tag{7}$$

Fig.5: SCS test structures

Comparison of the simulation results with measurements and full wave simulations revealed that the model obtained by simplifying the Van de Capelle model, lacked accuracy, both in resonance frequency and in impedance level. The resonance frequency, for example, could be 13% off, making the model unsuitable for use in an optimisation shell to generate an initial design. Like Duffy and Gouker in [8], we noticed that we could shift the resonance frequency by scaling the length-extension. For our frequency-range of interest – 0.8 GHz to 2.4GHz (GSM and Bluetooth) – we had a number of test radiators constructed (see fig.5) of which we measured the return loss as function of frequency. Since we observed a near-perfect agreement between measurements and simulations performed with ANSOFT's HFSS$^{©}$, we used the latter to generate data for a wide range of SCS radiators with different heights and widths, using the dimensions of a subset of the test structures as starting points. The length extension scaling function we obtained for our SCS radiator was not as straightforward as the one found in [8] for cavity backed microstrip antennas. However, for the range of interest, the function appears to be frequency- independent. The SCS length extension, obtained by LevenbergMarquardt curve fitting [9] is given by:

$$\Delta l_{SCS} = \xi_6 \Delta l \qquad (7)$$

$$\xi_6 = 1.6758(h/W)^{-0.1816} - 0.0931(h/W)^2 \\ + 0.8151(h/W) \qquad (8)$$

where Δl is given by (1).

For the impedance transformer we obtained a similar scaling function:

$$n_{SCS} = \alpha n \qquad (9)$$

$$\alpha = 0.6159(h/W)^{-1.3291} - 0.0697(h/W)^2 \\ + 0.3924(h/W) \qquad (10)$$

where [6]:

$$n = \sqrt{1 + 10\frac{h}{\lambda_0}} \qquad (11)$$

and the probe impedance is given by [5]:

$$Z_{feed} = -j\frac{\mu_0 h}{2\pi}\left(\ln\left(\frac{k_0 D}{4}\right) + 0.5772\right) \qquad (12)$$

where D is the diameter of the probe.
One has to be aware, however, that the scaling function of (10) for the impedance transformer ratio, rapidly looses accuracy for values of $(h/W) > 5$.
Some typical examples of the modified Transmission Line Method, applied to test radiators not used in the curve fitting process are shown in fig. 6. Since the model assumes the existence of an infinite ground plane, in the measurements, the test structures were mounted on a cupper plate of 40cm x 40cm.

Genetic algorithm optimisation
The number of parameters to be varied in our current radiator (in order to obtain the required antenna characteristics) is rather limited. We only have (with reference to fig. 4) W, h, L_1 and L_2 at our

Fig.6: Return loss vs. frequency for two SCS radiators.
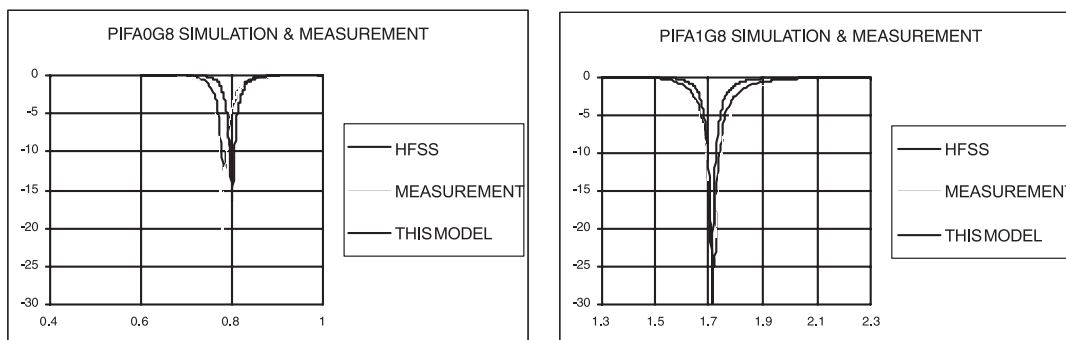
Fig.7: . Elements of Genetic Algorithm optimisation

disposal. It is anticipated though, that with the size reduction measures as shown in fig.1 and fig.3, the number of parameters will grow significantly. Therefore the need exists for a multi-parameter, constrainted optimisation method, preferably independent of any starting values supplied; i.e. a global optimisation method. Given these requirements, a Genetic Algorithm (GA) solution is particularly useful [10, 11], also since the software implementation of a general purpose GA -engine is very straightforward.
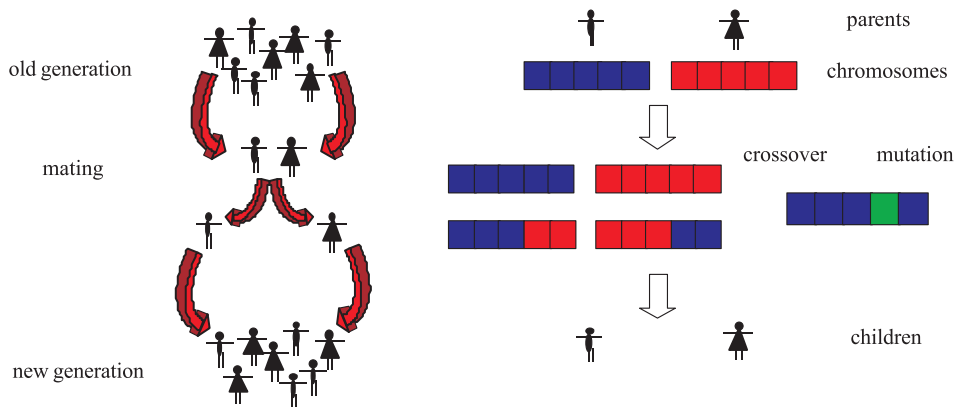
Genetic Algorithms are optimisation methods based upon the principles of natural selection and evolution. Concepts used in the optimisation process are: *Genes, chromosomes, generations, populations, parents, children and fitness*. A gene is a coded version of one of the parameters of the problem. A possible coding is a binary coding, making the *gene* a string of "zero's" and "one's". A *chromosome* is a series of *genes* and is thus a solution of the problem. The *gene* is also known as the *individual*. A *population* is a set of *indivuduals*. A *generation* is a *population* iteratively formed from the previous one. A *parent* is an *individual* from the previous *generation*; a *child* is an *individual* of the current generation. *Fitness* is a number assigned to an individual and a measure of "how good" this *individual* is.

In a typical GA optimisation problem, a starting population is created (randomly). In our antenna problem, where we want to find the length, height, width and probe position that give the smallest return loss at a chosen frequency or in a chosen frequency band, this population consists of sets of lengths, heights, widths and probe positions. Every individual from this population gets a fitness assigned. Here, this fitness could be the return loss at the chosen frequency, or the return loss over a frequency band. Next, parents are selected from the population (different selection proces ses exist) and by means of crossover and mutation children of a new generation are created. In the crossover process, parameters of two antenna configurations are intermixed. In the mutation process, one or a few of the parameters changes randomly. The process is depicted in fig. 7, for a five-parameter problem [10].

To test the feasibility of using the modified TL Model with a GA optimisation for generating designs to be fine –tuned by our full wave solver, we have performed a number of tests. The results of two of them will be shown. At first we aimed for resonance at 1.8 GHz. Fig.6 shows that iteratively employing ANSOFT's HFSS[©] by hand, resulted in

Fig.8: Optimisation results
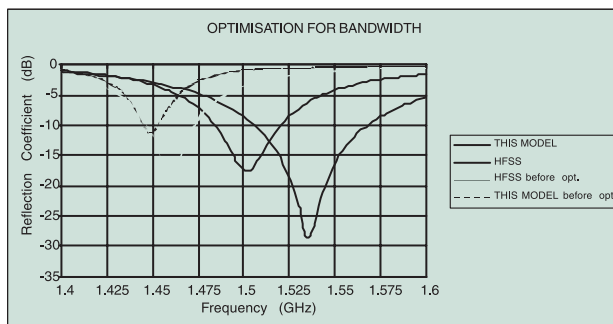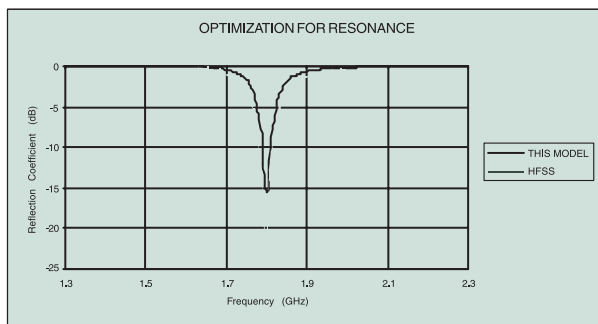
an antenna, resonant at 1.7 GHz. The result of the optimisation process is shown in fig.8. Secondly, our aim was a broad bandwidth around 1.5 GHz. The results of this optimisation process are also shown in fig.8.

The results clearly show how the fast but reduced accuracy analysis method can be used in combination with the GA optimisation – that requires many function evaluations - to generate an initial design. Both designs were obtained within minutes using a PC with a 450 MHz processor. Even though the number of parameters for this radiator is still very low, the time saving in the initial stage of an antenna design is considerable. It is remarkable that even with this low number of parameters at our disposal and working with a resonant structure, we can (though slightly) improve the bandwidth.

Cavity model for curved SCS-radiator

Of the two possible curved SCS antennas, the one depicted in fig. 9, where the strip is wound around the cylinder (as opposed to positioned in the axial direction), is the most challenging one.

It is not possible to translate the results of the planar modified Transmission Line Model directly to the circular cylindrical situation. The generalised transmission line model [12, 13] though can be easily adapted to the situation of the curved SCS, but requires an accurate calculation of the slot admittances, both the radiating one and the two nonradiating ones. It is therefore that we have chosen to exploit the cavity model, as done in [2] for a planar quarter wave microstrip antenna. We have chosen for the option where all the losses are lumped into an effective dielectric loss tangent [14,

fig 9:   Cylindrical rectagular microstrip antenna

15], leading to the following expression for the input impedance, with reference to fig.9:

$$Z_{in} = \frac{b-a}{2\pi\varepsilon_0} \sum_{m=0}^{\infty} \sum_{n=0}^{\infty} G_{mn}(\Delta\varphi, \Delta z) \Psi^2_{mn}(\varphi_1 + \varphi_0, z_0) \cdot$$
$$\frac{\delta_{eff} f^3 - j f(f^2 - f_{mn}^2)}{\delta_{eff}^2 f^4 - (f^2 - f_{mn}^2)^2} \tag{13}$$

$$G_{mn}(\Delta\varphi, \Delta z) = \sin\left[\frac{(2m+1)\pi\Delta\varphi}{4(\varphi_2 + \varphi_3)}\right] \sin\left[\frac{n\pi}{2W}\Delta z\right] \tag{14}$$

$$\Psi_{mn}(\varphi, z) = \frac{\mathcal{X}_n}{\sqrt{b(\varphi_2 + \varphi_3)W}} \cdot$$
$$\cos\left[\frac{(2m+1)\pi}{2(\varphi_2 + \varphi_3)}(\varphi - \varphi_1)\right] \cos\left[\frac{n\pi}{W}z\right] \tag{15}$$

$$f_{mn} = \frac{1}{2\sqrt{\varepsilon_0\mu_0}}\left[\left\{\frac{(2m+1)}{2b(\varphi_2 + \varphi_3)}\right\}^2 + \left\{\frac{n}{W}\right\}^2\right]^{\frac{1}{2}} \tag{16}$$

further;

$$\mathcal{X}_n = \begin{cases} 2 & n \neq 0 \\ \sqrt{2} & n = 0 \end{cases} \tag{17}$$

and:

$$\text{sinc}(x) = \frac{\sin(x)}{x} \tag{18}$$

The determination of the effective loss tangent as function of frequency appears to be critical in the determination of the input impedance using the cavity model. A fast determination of this parameter is still being investigated. The fringe fields can be accounted for by applying the same scaled length extension function (1)-(8) as used in the modified Transmission Line Model. For the test antennas shown in fig. 5, the resonance frequencies were calculated with a planar cavity model and with ANSOFT's HFSS©. The results are shown in table 1.

To show the validity of the cavity model for analysing curved microstrip antennas, we have used the cavity model to analyse a standard half wave microstrip patch antenna, adapting the method of
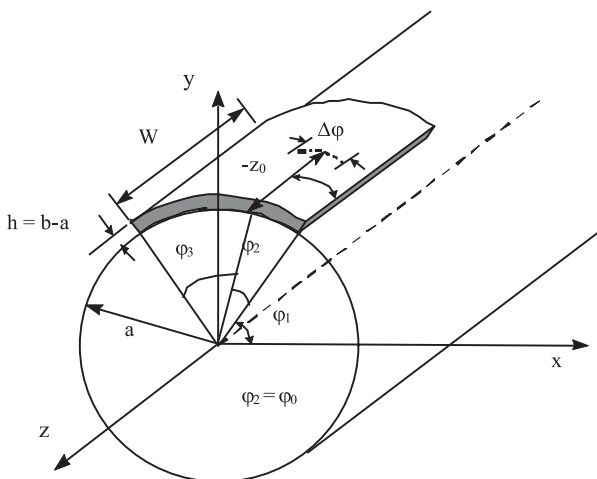
Table 1: Resonant frequencies for lanar test antennas

ANTENNA	HFSS©	Mod. Cav. Model
SCS-0G8	0.784 GHz	0.799 GHz
SCS-1G5	1.46 GHz	1.45 GHz
SCS-1G8	1.72 GHz	1.71 GHz
SCS-2G0	1.92 GHz	1.88 GHz
SCS-2G4	2.34 GHz	2.35 GHz

Dielectric constant	h (cm)	a = 5 cm	a = 10 cm	planar antenna
1.06	0.0795	218.0 + j2.8 (204.7 + j2.5)	216.4 + j2.8 (212.1 + j2.5)	214.7 + j2.8 (214.7 + j2.5)
	0.159	246.8 + j2.4 (228.0 + j4.7)	243.1 + j2.4 (234.3 + j4.7)	239.5 + j2.5 (235.0 + j4.6)
2.32	0.0795	245.0 + j1.0 (246.8 + j1.8)	243.1 + j1.0 (233.9 + j1.8)	241.2 + j1.1 (217.9 + j1.8)
	0.159	317.6 + j9.7 (316.6 + j3.6)	312.8 + j9.6 (296.9 + j3.6)	308.1 + j9.5 (270.5 + j3.6)
9.8	0.0635	152.1 + j8.9 (192.7 + j0.6)	151.2 + j8.8 (186.8 + j0.6)	150.3 + j8.8 (180.0 + j0.6)

Table 2: Input impedance at resonance (Ohms) of the TM(10)-mode for a curved patch with $(a + h)(\varphi_2 + \varphi_3) = 4$ cm, $W = 3$cm and fed at $-z' = 1.5$ cm, $(a + h)\,\varphi_2 = 1$cm , $\Delta\varphi = 5$mm.

[15], but using the closed form expressions of Daniel et al. [16] for determining the effective loss tangent for a planar configuration. The expressions were rewritten for the circular cylindrical situation, taking the arc length over the patch as replacement for the rectangular patch length. The modal frequencies were adapted according to [17].

Input impedances for various structures are presented in table 2. The results of [15] are given in parentheses for comparison purposes. The table clearly shows the validity of the cavity model for this curved radiator.

Conclusions

The synthesis of miniature (conformal) antennas, using analytical models has been investigated. In order to perform this research, a Short Circuited Strip (SCS) antenna is introduced. This radiator will be the basis for future miniatureantenna designs. The analytical models, based on a-priori assumptions result in fast computer algorithms at the cost of a reduced accuracy. The idea to be verified is that it should be possible to use these fast reduced accuracy models in combination with a Genetic Algorithm optimiser (needing many function evaluations) to generate preliminary designs, to be fine-tuned with (much slower) 3D full wave electromagnetic solvers. The idea has been tested on Short Circuited Strip antennas and leads to the conclusion that it is possible to use reduced accuracy models in a global optimisation scheme to generate preliminary designs. The time saving in the antenna design process, especially at the start will be significant. The method will benefit from ongoing research in the development of reduced accuracy models for miniature antennas.

Based on the results for the planar SCS antenna and preliminary results for rectangular cylindrical microstrip antennas it is expected that the design strategy will work evenly well for curved radiators.

References

[1] T. Taga, "Analysis of Planar Inverted-F Antennas and Antenna Design for Portable Radio Equipment", in Analysis, Design, and Measurement of Small and Low-Profile Antennas, K. Hirasawa and M. Haneishi, Eds., Artech House, London, pp.161-179, 1992.

[2] S. Pinhas and S. Shtrikman, "Comparison Between Computed and Measured Bandwidth of Quarter-Wave Microstrip Radiators", *IEEE Transactions on Antennas and Propagation*, Vol. 36, No.11, pp.1615-1616, November 1988.

[3] P.C. Sharma, "Desegmentation Method for Analysis of Two-Dimensional Microwave Circuits", *IEEE Transactions on Microwave Theory and Techniques*, Vol. MTT-29, No. 10, pp.1094-1098, October 1981.

[4] A. van de Capelle, "Transmission-line Model for Rectangular Microstrip Antennas", in Handbook of Microstrip Antennas, J.R. James, P.S. Hall, Eds., Peter Peregrinus, pp.527-578, 1990.

[5] J.X. Zheng and D.C. Chang, "End-Correction Network of a Coaxial Probe for Microstrip Patch Antennas", *IEEE Transactions on Antennas and Propagation*, Vol. 39, No. 1, pp. 115-118, January 1981.

[6] B. Nauwelaers, "Een Analysemodel voor Roosters van Rechthoekige Microstripantennes", status unknown.

[7] M. Kirsching, R.H. Jansen and N.H.L. Koster, "Accurate Model for Open End Effect of Microstrip Lines", *Electronics Letters*, Vol. 17, No.3, pp.123-124, 5th February 1981.

[8] S.M. Duffy and M. A. Gouker, " A Modified Transmission Line Model for Cavity Backed

Microstrip Antennas", *Antennas and Propagation Society International Symposium*, 1997, IEE., Digest, Volume 4, pp.2139-2142, 1997.

[9] W.H. Press, B.P. Flannery, S.A. Teukolsky and W.T. Vetterling, "*Numerical Recipes, The Art of Scientific Computing*", Cambridge University Press, pp.523-528, 1988.

[10] J.M. Johnson and Y. Rahmatt-Samii, "Genetic Algorithms in Engineering Electromagnetics", *IEEE Antennas and Propagation Magazine*, Vol.39, No.4., pp.7-21, August 1997.

[11] J.M. Johnson and Y. Rahmatt-Samii, " An Introduction to Genetic Algorithms", in Electromagnetic Optimization by Genetic Algorithms, Y, Rahmatt-Samii and E. Michielsen, Eds., John Wiley & Sons, Inc., New York, pp.1-27, 1999.

[12] A.K. Bhattacharyya and R. Garg, "Generalised Transmission Line Model for Microstrip Patches", *IEE Proceedings*, Vol. 132, Pt. H, No.2, pp.93-98, April 1985.

[13] K.L. Wong, Y.H. Liu and C.Y. Huang, "Generalized Transmission-Line Model for Cylindrical-Rectangular Microstrip Antennas", *Microwave and Optical Technology Letters*, Vol.7, No.16, pp.729-732, Nov. 1994.

[14] K.R. Carver and J.W. Mink, " Microstrip Antenna Technology", *IEEE Transactions on Antennas and Propagation*, Vol. AP-29, No.1, pp.3-25, January 1981.

[15] K.M. Luk, K.F. Lee and J.S. Dahele, "Analysis of the Cylindrical-Rectangular Patch Antenna", *IEEE Transactions on Antennas and Propagation*, Vol. 37, No.2, pp.143-147, February 1989.

[16] J.P. Daniel, G. Dubost, C. Terret, J. Citerne and M. Drissi, "Research on Planar Antennas and Array: "Structures Rayonnantes"", *IEEE Antennas and Propagation Magazine*, Vol. 35, No.1, pp.14-38, Feb. 1993.

[17] J.R.James, P.S. Hall and Wood, "*Microstrip Antennas, Theory and Design*", Peter Peregrinus, London, p.100, 1981.

Authors

Hubregt J. Visser
TNO Industrial Technology
PO Box 6235, 5600 HE Eindhoven, The Netherlands
also:
Eindhoven University of Technology, Faculty of Electrical Engineering
PO Box 513, 5600 MB Eindhoven, The Netherlands

Jan Jonkergouw
TNO Industrial Technology
PO Box 6235, 5600 HE Eindhoven, The Netherlands

Jos C.J.M. Warnier
Eindhoven University of Technology, Faculty of Electrical Engineering
PO Box 513, 5600 MB Eindhoven, The Netherlands

A matrix-based polarimetric model for a CMB polarimeter telescope

J.P. Hamaker
ASTRON, P.O. Box 2, 7900 AA Dwingeloo,
Netherlands[1]

Introduction

Radio astronomy developed from observations of unpolarized flux and brightness using antennas with single feeds. For this purpose, a scalar representation of the radiation and the antenna /receuver system is fully adequate. Polarimetry evolved several decades later, as an afterthought one might say, and is accounted for in an approximate way as a first-order perturbation on the scalar equations. The extended equations have formed a basic tool of radio polarimetry ever since. Apart from being a mere approximation, this approach is inadequate in that it fragments the problem and deals with the parts in isolation: There is no grand picture – lengthy explanations appear in its place and important aspects got completely lost.

It may be possible nonetheless to get away with this approach even in the most daring and ambitious quest of measuring CMB polarization – but a rigorous approach is obvious to be preferred, if only to reassure oneself that nothing important has been overlooked. To this end, this contribution applies the matrix-based description of polarimetry (Hamaker 2000; see also Hamaker et al. 1996) in modeling a CMBP instrument (for which PLANCK served as an example).

This description is complete, clean, coherent and modular, showing the things that matter without the encumbrance of distracting detail that is so characteristic of scalar-based treatments. A clear conceptual distinction emerges between the signal as such and the way in which it may be represented; or, more or less equivalently, between the characteristics of the signal and those of the measuring equipment. Consequently, the analysis need not be narrowed down to a particular instrumental configuration (linearly/circularly polarized feeds, correlating or differencing receiver) until the point where the errors in a specific design must be considered.

Although the emphasis in this paper is on astronomical measurement of an extremely weakly polarized background signal, the matrix formalism is universally valid and may be brought to bear on many other situations in which a proper description and understanding of polarization phenomena are important.

The matrix formalism

I give here a very brief summary of the matrix formalism. See Hamaker Bregman and Sault (1996) and the first sections of Hamaker (2000) for the full story.

Signal Vector, Jones and Coherency Matrices

The amplitude of the electric radiation field propagating in the z direction is a vector

$$e = \begin{pmatrix} e_p \\ e_q \end{pmatrix} \tag{1}$$

where p and q are two-dimensional cartesian coordinate axes. Commonly used systems are geometric xy and circular rl coordinates. We will use the former exclusively.

Along its path, this signal encounters linear transformations; we represent each by a matrix multiplication

$$e' = J\,e\,, \tag{2}$$

where the 2 x 2 matrix J is known as a *Jones matrix*. For a chain of transformation stages labeled 1, 2, ... , N, the overall Jones matrix is the product of the stage matrices in reverse order:

$$J = J_N \dots J_2 J_1 = \textstyle\prod_k J_k \tag{3}$$

In this note it is understood that the factors in a product $\prod_k J_k$ always appear in descending order of k. Polarization of the radiation is characterised by the auto- (powers) and cross-covariances of the field components, which are the elements of the *coherency matrix*

$$C = <e_P e_q^\dagger> \equiv < \begin{pmatrix} e_P e_P^* & e_P e_q^* \\ e_q e_P^* & e_q e_q^* \end{pmatrix} > \equiv \begin{pmatrix} e_{pp} & e_{pq} \\ e_{qp} & e_{qq} \end{pmatrix}, \quad (4)$$

where the dagger superscript indicates hermitian transposition and the angle brackets <> represent time averaging. Note the use of single indices for field components, double indices for matrix elements. The diagonal elements represent the powers in the e_{pp} and e_{qq} fields and each contain one half of the unpolarized part of the radiation.

Also note that the electric field is measured in a single point rather than in two interferometer elements as in the references; consequently, the coherency matrix is hermitian and contains only 4 independent parameters. This is also true for the output of any signal transformation; this requirement may serve as a simple check on the correctness of the analytical expressions and approximations to be developed below.

From (2) and (4) it immediately follows that the effect of a Jones matrix J on the coherency matrix is given by (Hamaker 2000)

$$C' = JCJ^\dagger . \quad (5)$$

Stokes Parameters: Intensity and Polvector

The *Stokes vector* (*I, Q, U, V*) is an alternative representation of the coherency matrix; in *xy* coordinates:

$$\begin{pmatrix} I \\ Q \\ U \\ V \end{pmatrix} \equiv \frac{1}{2} \begin{pmatrix} e_{xx} + e_{yy} \\ e_{xx} - e_{yy} \\ e_{xy} + e_{yx} \\ -i(e_{xy} - e_{yx}) \end{pmatrix} \quad (6)$$

Conversely

$$C = \begin{pmatrix} I+Q & U-iV \\ U+iV & I-Q \end{pmatrix} \quad (7)$$

In the present context the Stokes parameters are intrinsically real. For an unpolarized source, C is a multiple of the indentity matrix I. The polarized part of the radiation is represented by the other three parameters which form the *polvector*

$$p \equiv (Q, U, V) \quad (8)$$

that resides in an abstract polvector space of its own. (The term 'polvector' was introduced by Hamaker (2000); a closely related concept is that of the Poincaré é sphere, which is the locus of the normalized polvector p/I for a fully polarized signal.)

The values of I and p as functions of celestial position is what CMBP experiments are supposed to measure. V is assumed to be zero: $p = (Q, U, 0)$.

Scalar and Vector Parts of 2 x 2 Matrices

The Stokes representation is not restricted to coherency matrices. Equation (7) applies to any matrix and we may thus generally define the *scalar* and *vector parts* of a matrix, corresponding respectively to I and p above. This gives rise to an interesting and valuable geometrical interpretation of the matrices and their products and transformations (Hamaker 2000) – which is, however, outside the scope of this paper.

In physical terms, the scalar part of a Jones matrix simply scales the coherency without altering its relative polarization p/I. The vector part is responsible for rotations of the polvector and for mutual conversion between the unpolarized and polarized parts of the coherency (Hamaker 2000).

Coordinate Systems

The (*Q, U, V*) coordinate axes in polvector space may represent any Cartesian frame. The conventional choice is to let positive Q represent a signal whose preferred direction of vibration is along the x axis of our physical coordinates, and positive U along position angle $+\pi/4$ (Hamaker and Bregman 1996).

It is natural (although not necessary) to align one's coordinates with an axis of symmetry of the instrument. E.g. for the PLANCK LFI, an obvious choice is the symmetry plane of the dual-reflector system. Such choices are a matter of convenience and we may even use different frames for different parts of our systems, interspersing transformations where necessary. For example, if the OMT were to have a symmetry plane that is different from that of the optics, one might use two different coordinate systems joined by a geometric rotation.

The Norm of a Matrix

A a measure to compare the relative magnitudes of matrices we use the Euclidian or Frobenius norm

$$\|A\| = \sqrt{\sum_{jk} |a_{jk}|^2} = \sqrt{\operatorname{Tr} AA^\dagger}. \quad (9)$$

From this definition it follows that all elements of A are smaller in absolute value than its norm. The norm has the useful property that

$$\|A\| \, \|B\| \le \|AB\| \tag{10}$$

The adjectives *large* and *small* for matrices are to be understood in terms of this norm. The unit for comparison is $\|\mathbf{I}\| = 2$.

Frequency Dependence

In principle, all our matrices are frequency-dependent. Conceptually, the system should be considered to consist of a set of independent and mutually incoherent parallel channels spread over the system bandwidth (Hamaker et al. 1996). The output coherency is then the sum of the channel outputs and overall system behaviour cannot be described in terms of a single chain of Jones matrices. For each specific instrument, this aspect must be separately investigated.

Jones versus Mueller matrices

It is also possible to describe the signal transmission in terms of linear transformations of the Stokes vector; the corresponding 4 x 4 multiplier matrices are known as *Mueller matrices*. Note, however, that the Stokes parameters represent powers; they are therefore unsuitable for describing the superposition of (partially) coherent signals. Also, the relation of the Mueller matrices to the underlying Jones matrices that describe the hardware is rather indirect (Hamaker et al. 1996).

Error analysis

Generic System Model

Figure 1 is the schematic that we will use in our analysis. It shows no more detail than we actually need at this point and is meant only as a reference for the error analysis to follow. In this chapter, we will use the generic symbol Jk rather than the more specific symbols in the figure.

Error Types

In the ideal system, the output coherency would be a scaled replica of the input, leaving only the scale factor to be determined. Any deviation from this condition is what we call a (polarimetric) *error*.

There are two types of errors to be considered. Errors in the Jones matrices multiply the signal and coherency, producing an error in the output coherency that is proportional (in a matrix sense) to the

input; we call such errors *multiplicative*. Other errors result from *interfering signals* entering the system; they cause an offset in the output coherency that is *additive*. (Strictly, interfering signals from the target source produce a multiplicative error if the differential delay is small enough; this case is covered by Sect. "Coherent Superposition")

Multiplicative Errors
Scalar matrices

Ideally, each of our Jones matrices should equal $\mathbf{I}$, the identity matrix or a scalar multiple thereof. Such matrices both add and multiply like scalars and may therefore be identified with them. A scalar matrix merely scales the signal vector and coherency matrix. Furthermore for a scalar 2 x 2 matrix $M = m\mathbf{l}$

$$\det M = \det m\mathbf{l} = m^2; \; M = \mathbf{I}\sqrt{\det M} \tag{11}$$

Figure 1: A representative schematic block diagram of a typical CMBP telescope. The essential components of the primary signal path are shown in the left column. Representative prototypes of various types of spurious paths are indicated to the right.
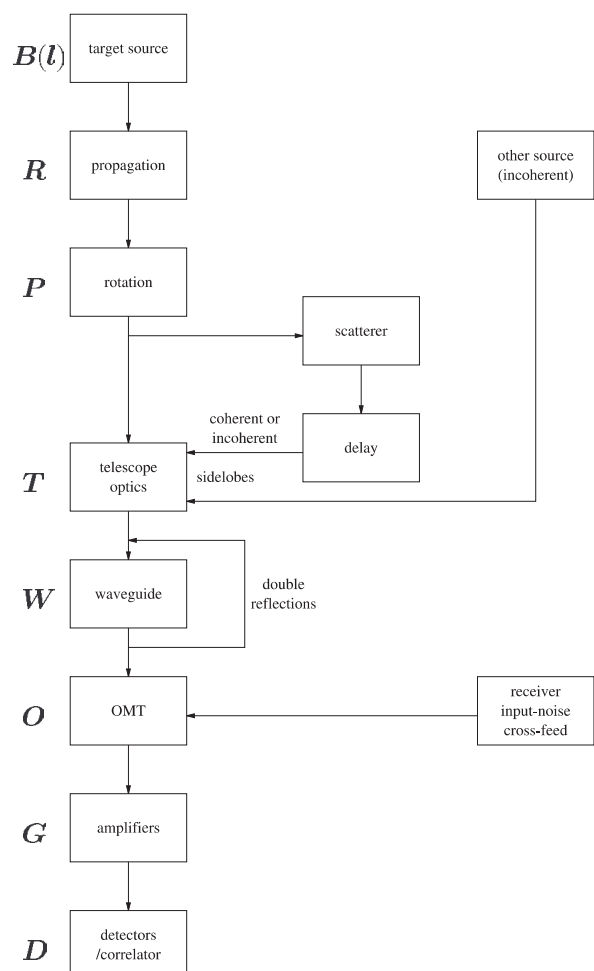
True Jones Matrices

The Jones matrices in our system are designed to deviate little from the ideal of a scalar matrix; we may represent them as

$$J_k = \sqrt{\det J_k}\,(\mathbf{I} + \delta J_k) \tag{12}$$

where δJ_k is small. We may also say that J_k is *nearly scalar*. The rationale for this decomposition is that products with scalar matrices are commutative; by swapping factors in such a product we obtain expressions that are more transparent and interpretable.

More precisely, δJ_k is composed of a small, strictly constant errer $\overline{\delta J}_k$ and an even smaller *variable error* $\widetilde{\delta J}_k$ making

$$J_k = \sqrt{\det J_k}\,(\mathbf{I} + \overline{\delta J}_k + \widetilde{\delta J}_k). \tag{13}$$

In the same way we write the sky coherency as

$$C = \sqrt{\det C(l)}\,(\mathbf{I} + \delta C(l)). \tag{14}$$

I are the pointing coordinates; we will not carry them explicitly in the sequel.

In analysing polarimetric system performance, we may ignore the scalar multipliers and concentrate on the error terms in the parentheses. The constant errors are of order 10^{-2}; the variable errors are at least another two orders smaller ($10^{-6} - 10^{-4}$), but they may be well above the target accuracy which is of order $10^{-7} - 10^{-6}$ of the brightness level of 2.7K. If they are, the variations will have somehow to be calibrated.

Multiplicative-Error Model

The system Jones matrix J (without a subscript) is

$$J = \prod_k J_k = \prod_k \sqrt{\det J_k}\,(\mathbf{I} + \overline{\delta J}_k + \widetilde{\delta J}_k). \tag{15}$$

Considering the magnitudes of the previous section, we may simplify the equation. In the product $\prod J_k$

- All products involving only fixed errors $\overline{\delta J}_k$ add up to a new fixed error $\overline{\delta J}$. It is dominated by the linear term $\sum \overline{\delta J}_k$ whose order of magnitude is that of the individual $\overline{\delta J}_k$.
- All products involving more than one variable term may be neglected.
- All products involving a mixture of fixed and variable error terms are much smaller than the variable terms themselves and may be neglected.

The remaining terms are

$$J \approx \sqrt{\det J}\,(\mathbf{I} + \overline{\delta J} + \sum_k \widetilde{\delta J}_k). \tag{16}$$

We may use the shorthand $\widetilde{\delta J}$ for the third term to write J in the standard form of (13) when this is convenient.

Output Coherency

From (5), (14) and (16), the output coherency becomes

$$C' = JCJ^\dagger \approx |\det J|\,(\mathbf{I} + \overline{\delta J} + \widetilde{\delta J})\,\sqrt{\det C}\,(\mathbf{I} + \delta C) \cdot (\mathbf{I} + \overline{\delta J} + \widetilde{\delta J})^\dagger \tag{17}$$

We may again neglect products involving two or more error terms and/or δC, leaving

$$C' \approx |\det J|\,\sqrt{\det C}\,(\mathbf{I} + \delta C + 2\mathrm{He}\,\overline{\delta J} + 2\mathrm{He}\,\widetilde{\delta J}) \tag{18}$$

where the symbol He stands for the *hermitian part of*.

Possible Refinements

The model may be refined by including certain second-order products or even more. At present I see no justification for doing this.

Additive Errors

Additive errors may originate from the target source itself through stray paths; such paths are formed by

- beam sidelobes picking up radiation scattered off the satellite structure;
- fractions of the signal being reflected backward and then forward again in the telescope optics and/or the waveguide system.

Depending on the differential delay, the error signal may be coherently or incoherently related to the target signal.

Other sources may also contribute an error signal: Both the sky and radiation from the satellite itself are picked up by beam sidelobes. These signals are always incoherent with the target source.

Coherent Superposition

In the coherent case, the target and error signals add. The error signal is coherently derived from the

target and therefore representable by the latter multiplied with an error Jones matrix J', so we get

$$e'' = Je + e' = (J + J')\, e \tag{19}$$

The net effect is that of adding one or more (relatively small) error terms to the system Jones matrix J; they may contain both fixed and variable parts. One particular possible source of variation are moving parts of the satellite.

Incoherent Superposition

For incoherent superposition, it is the *coherency matrices* that add. We consider the point where the superposition happens. The target source's coherency is JCJ^t and the interfering coherency $J'C'J'^t$. Then the output C'' becomes

$$C'' = JCJ^\dagger + J'C'J'^\dagger \tag{20}$$

To estimate the relative magnitude of the error, we may approximate J and C' by their scalar parts to get

$$C'' \approx \left|\det J\right| \left(C + \left|\det J\right|^{-1} J'C'J'^\dagger\right) \tag{21}$$

There are too many variables to allow a general conclusion. One must consider each possible interference source separately, taking into account its strength C' and the path J' through which its enters.

Summary of Results

It may be useful at this point to summarise what we have learnt.

- The system Jones matrix is given by (16). It contains a fixed and a variable error term, both of which are represented with appropriate accuracy by the sums of the corresponding errors in the component Jones matrices.
-
- The output coherency is given by (18). It contains a scaled replica of the input coherency C, contaminated by the input intensity $c\mathbf{I}$ multiplied by twice the hermitian part of the error terms in the system Jones matrix.
- Spurious signals from the target source entering with a small differential delay contribute extra multiplicative error terms to (16).
- Spurious signals from the target source entering with a big delay as well as signals from other sources contribute addytive error terms per (20) and (21) to the coherency.

- The latter two types of error may also contain fixed and variable parts; they must be analysed for each individual source of interference.

This is as far as the generic analysis will carry us. At this point, the details a specific instrument configuration and its constituent parts come into play.

Antenna model

By the antenna I understand the optics that converts the incident plane waves from the entire sky into a single guided wave. This is the input operation common to all instruments. The antenna consists of a feed horn and a(n optional) (set of) reflector(s). The properties of these components are so intertwined that the only reasonable way to model them is through a single Jones matrix T that is a function of spatial coordinates l. The antenna integrates the incident coherency $B(l)$ over the sky with T as Jones matrix:

$$C' = \int d\Omega\; T(l)\; B(l)\; T^\dagger(l) \tag{22}$$

In decomposing this integral it is convenient to split T in its scalar and vector parts:

$$T = t\mathbf{I} + \delta T, \quad t(l) = \tfrac{1}{2}\operatorname{Tr} T(l). \tag{23}$$

Then

$$C' = \int d\Omega\; (t\mathbf{I} + \delta T)\; B\,(t\mathbf{I} + \delta T)^\dagger \tag{24}$$

$$= \int d\Omega\; [|t|^2\, B + 2\mathrm{He}\; (t\, B\,\delta T^\dagger) + \delta T\, B\,\delta T^\dagger \tag{25}$$

The first term in the integrand is the weighted matrix brightness; this is what an ideal scalar or polarizationfree antenna ($T = t\mathbf{I}$; $\delta T = 0$) would yield.

The argument of the second term is the weighted cross-covariance of the brightness and the beam's vector part, with t (i.e. the scalar part of the *voltage* beam) acting as the weight factor.

The third term, being quadratic in δT, is second-order small over the entire beam. However, unlike the similar second-order terms in Sect. "Multiplicative-Error Model" it is not constant since it depends on the position of the sky relative to the telescope. Although smaller than the middle term, it must be retained and analysed; in a complete analysis, the split (23) is not necessarily very useful.

One may also interpret (25) as an expansion of C′ in powers of the relative instrumental polarization $\delta T(l)/t(l)$:

$$C' = \int d\Omega \; |t|^2 \left[B + 2He \; B(\delta T^{\dagger}/t) + \delta T/t \; B(\delta T/t)^{\dagger} \right]$$
(26)

By design, the beam should be weakly polarized in the main lobe – i.e. $\|\delta T/t\| \ll 1$ where $|t|$ is large. In the sidelobe region δT is an oscillating function of l of the same order of magnitude and, since $|t|$ is small, sidelobes may be strongly polarized.

The telescope output is the convolution over the entire sphere of the beam with the sky coherency. It is dominated by the main beam, but the sidelobe contributions are nonnegligible at the accuracy levels required; some kind of deconvolution will be necessary. In my opinion, this matter needs to be studied with greater care than may have been done so far; for this, the equations of this section provide a better starting point than representations in terms of scalar formulae (e.g. Carretti et al. 2001).

Rotation and conversion transformations

Any matrix J can be represented (Hamaker 2000) as the product of a scale factor with unimodular unitary and positive-hermitian matrix factors:

$$J = cHY.$$
(27)

(A unimodular matrix has a unity determinant; unitary matrices are the matrix equivalent of scalar phase factors, positive-hermitian matrices the equivalent of positive numbers;)

Applying this to the Jones matrix J in the interferometer equation (5) we get

$$C' = JCJ^{\dagger} = c \; H \; (YCY^{\dagger}) \; H^{\dagger}.$$
(28)

The inner transformation $X = YCY^{\dagger}$ leaves the Stokes intensity I invariant, since for a unitary matrix $YY^{\dagger} = I$. Furthermore it can be shown to *rotate the polvector* in its abstract polvector space. The rotation axis and angle are functions of the four elements of Y; a detailed discussion is given in Hamaker (2000).

The outer transformation $C' = HXH^{\dagger}$ effects a mutual conversion of power between intensity I and polvector p without changing the latter's orientation – the transformation is said to be *rotation-free*. Again, the precise form of the conversion depends on the elements of the transformation matrix (Hamaker 2000).

Since J is nearly scalar (cf. Sect. 3.3.2), so are Y and H; in other words, Y represents a rotation over a small angle and H converts a small fraction of I. Since $p/I \ll 1$ the inverse conversion is negligible.

References

E. Carretti, R. Tascone, S. Cortiglioni, J. Monari, J. and M. Orsini 2001: "Limits due to instrumental polarisation in CMB experiments at microwave wavelengths." *New Astronomy* 6, 173-187, 2001.

J.P. Hamaker, J.D. Bregman and R.J. Sault 1996: "Understanding Radio Polarimetry, I: Mathematical Foundations". *Astron. and Astrophys. Suppl.* 117, 137-1467, 1996.

J.P. Hamaker and J.D. Bregman 1996: "Understanding Radio Polarimetry, III: Interpreting the IAU/IEEE definitions of the Stokes parameters". emphAstron. and Astrophys. Suppl. 117, 161-165, 1996.

J.P. Hamaker 2000: "Understanding Radio Polarimetry, IV: "The full-coherency analogue of scalar self-calibration: Self-alignment, dynamic range and polarimetric fidelity". *Astron. and Astrophys. Suppl.*, 143, 515-534, May I, 2000.

Semi-active Ka-band reflectarray antenna

John A.J. de Groot [1], *Jos T.C. Duivenvoorden* [2]
Thales Netherland B.V., P.O. Box 42, 7550 GD Hengelo (Ov.),
The Netherlands
(1) Email: john.degroot@nl.thalesgroup.com
(2) Email: jos.duivenvoorden@nl.thalesgroup.com

Introduction

Antenna front-ends for modern active phased array radars and communication systems are characterised by a large operational bandwidth and the ability to scan over a large angular area. Cost drivers for such antennas are active components including GaAs MMICS. If some reduced performance is acceptable, much less expensive alternatives for active phase array antennas are reflectarray antennas. The work presented here describes design, production and testing of a semi-active Ka -band reflectarray, developed by Thales Nederland B.V. The antenna consists of a feedhorn in front of a thin flat reflectarray multi-layer printed circuit board. The toplayers consist of integrated RF radiator and phase shifter elements. PIN diode switches control reflection phase. The backlayers are for digital control, data distribution and dc power distribution.

Design of the reflectarray antenna concentrated on antenna efficiency, particularly for the phase shifter design. At Kaband frequencies many materials have relatively high loss tangent. Applicable PIN-diode switches introduce reduced switching due to series resistance and capacitive RF currents. The principle of operation is chosen to minimise loss mechanisms. A finite element software tool is used to optimise the dimensions of the reflectarray elements. Results are validated by measurements on small samples in a waveguide simulator. After several design iterations a prototype reflectarray antenna is put into production and tested afterwards. The study is presented with photos of the antenna hardware within and after production, as well as the nearfield and farfield measurement results.

Problem description

Three types of reflectarrays can be distinguished: passive (fixed beam and passive reflection), semi-active (electronic beamsteering and passive reflection) and active (electronic beamsteering and amplified reflection). This paper concerns the development of a semi-active Ka-band reflectarray demonstrator. The demonstrator must prove the semi-active reflectarray antenna concept. This paper gives a brief overview of the presentation contents.

Principle of operation

Phase shifter elements are the fundamental parts of a reflectarray antenna. One of the key features is how the individual elements are adjusted to scatter the desired phase. Proper characteristics are: fast switching time, phase states with uniform distribution, low loss, wide band operation, good scan performance, low production cost and compatible with a building block design philosophy. This paragraph describes phase shifter loss issues: loss in general, material losses, quantisation loss and loss in switches.

Phase shifters inhibit sensitive phase influence operating at and around resonance frequencies. Therefore it seems attractive to design when large phase changes are required. However at resonance, current and electric field excitations are very intense. Therefore the loss is relatively high and the operating bandwidth small. The remedy is simple: design phase shifters in non-resonance zones. Out of resonance there are regions where phase states can be controlled properly. Some types of Frequency Selective Surfaces [6, 7] also have such regions: semi -reflective-inductive, non-reflective-transparent and semi-reflective-capacitive.

Another advantage is that phase shifters, operating out of resonance, are more robust for production and material tolerances compared to phase shifters operating around the resonance frequency.

The loss tangent, which depends on the dielectric constant of the used material and the operating frequency, states material losses. The default relation is that the loss tangent increases with the frequency. Above a certain frequency the loss tangent reaches impracticable values. Materials should be selected for frequency bands where the loss tangent is low. Electric field distributions, in general, can be seen as a set of propagating and evanescent modes. Besides the propagating fundamental mode, excited modes around or even below cut-off are contributing to the loss significantly. Decreasing the dielectric constant can reduce the number of propagating modes in the substrate. The loss tangent of the dielectric substrate is the main factor in this loss mechanism.

One design goal for the phase shifter is to change reflection phase gradually when the RF switches are toggled. This gives the least quantisation loss with the available number of switches. Important here is the interaction between the phase state distribution and the switch impedances [5]. The impedance of the switch can be modeled by an equivalent circuit of the RF switch. When typical values are chosen, the on-state impedance is close to real (resistive) and the offstate impedance is negative imaginary (capacitive). Therefore the RF switch is often modeled as R_on (on-resistance) in on-state and C_off (off-capacitance) in off-state. The R_on and C_off combination is crucial in the switching mechanism. When R_on and C_off are high, the discrimination between on- and off-state is small. Such equipped phase shifters should be very sensitive to changes of RF switch impedance to provide proper phase states. When R_on and C_off both are low, the phase shifter can be more robust and good switch is obtained. Another loss mechanism is cased by phase errors due to quanti-

sation. Phase errors lead to reduction of antenna gain AG [4] and are preferably minimised,

$$\Delta G \approx 1 - \sigma_\Phi^2 = 1 - \frac{\pi^2}{3 \cdot 2^{2p}} \qquad (1)$$

where σ_Φ is the RMS phase error and p the effective number of bits. Equation (1) becomes valid for apertures which contain a large amount of phase shifters.

For loss in switches R_on is the main parameter. Actual loss is dependent on the current fraction through R_on and C_off. The RF switch parameters and phase shifter design determine this, because the combined parameters determine the currents. There is a minimum loss design for each type of RF switch. Manufacturers of RF switches are involved in such study. The simulation tool High Frequency Structure Simulator HFSS [1] is used, to demonstrate theoretically, the principle of operation before production. After sample production the model is optimised leading to the final design. Loss issues are found together in the gain balance:

Production of the antenna hardware

The antenna hardware consist of the following steps: etching of separate layers, drilling, via metalization, layer integration, bareboard testing, placement of components and fixation of the board in a frame. The sequence of production steps is matched to the specific interconnection topology. The bare board reflector contains 9 conductor films, which are connected by 38.784 through vias, blind vias and micro vias. At first, the layers are pressed together where blind vias are still accessible for drilling and metalization (Figure 1). After that, the separate multilayers are pressed together and remaining vias are created. The aspect ratio of most vias is 1:7 (0.25mm. diameter, 1.8mm. length).

After layer production, the board is tested by the use of a bareboard tester. Within a selected region of 4224 phase shifters, more than 99% of the phase shifters appeared operational. Results are used for feedback into the simulation model, so that

Table 1: Gain balance of the reflectarray antenna

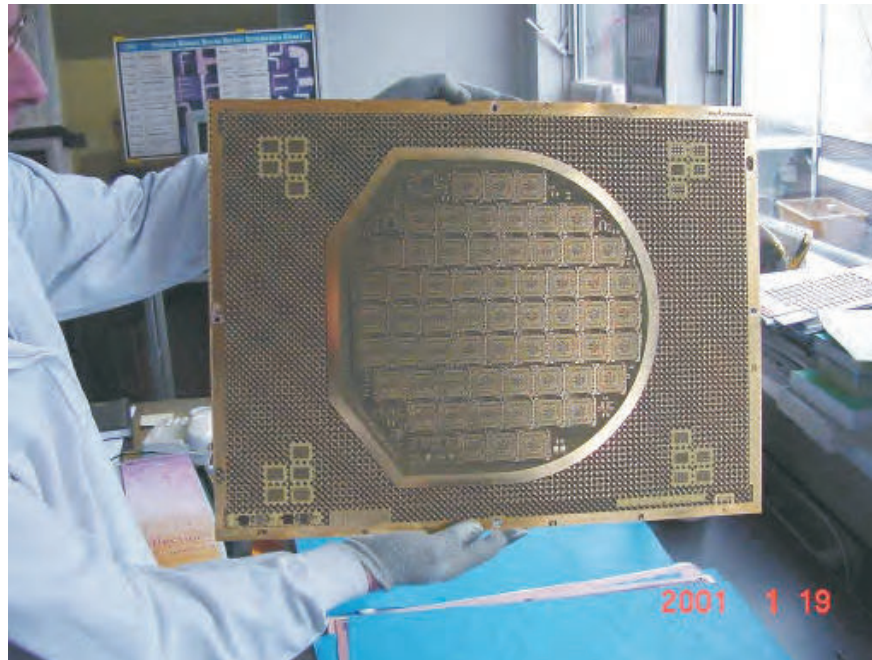|		
Surface gain	40.9 dB	4*pi*S/lambda^2 with S=0.72 m^2, λ=3e8 m•s^{-1}/35 GHz
Aperture efficiency	-1.5 dB	70% taper efficiency
Spillover, VSWR, feed loss	-0.6 dB	
Quantisation loss	-1.1 dB	1.95 bits
Phase shifter loss	-2.0 dB	Waveguide simulator
Estimated Gain	35.7 dBi	

Figure 1: Layer production

electrical impact of defects can be studied. The assembly of the components on the board is performed by the use of an automatic pick-and-place process. Each phase shifter includes 2 flip-chip PIN diodes mounted to the board by means of conductive adhesives. The electronic control circuitry is soldered on the backside. Wiring for the power supply and data is connected and the board is fixed on an aluminium frame (Figure 2).

Testing and results

A measurement setup with a waveguide simulator is used for the measurement of reflectarray samples. It offers an opportunity to measure the infinite array behavior with inexpensive small size hardware of a few antenna elements. Figure 3 shows some measured results of a 2-bit electronically controllable reflectarray sample inside a multi-mode waveguide simulator [2]. Three angles of incidence are measured instantaneously with this waveguide simulator.

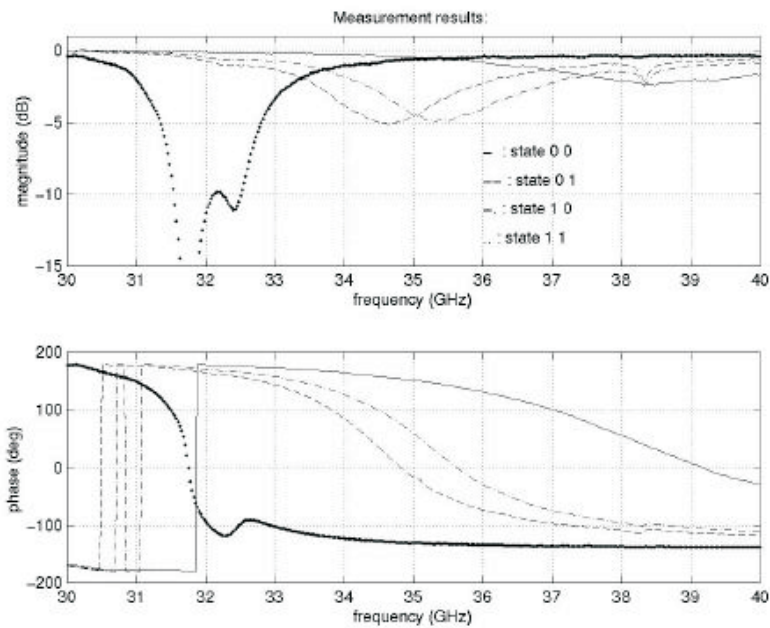Figure 2: The complete reflectarray antenna in the aluminum frame
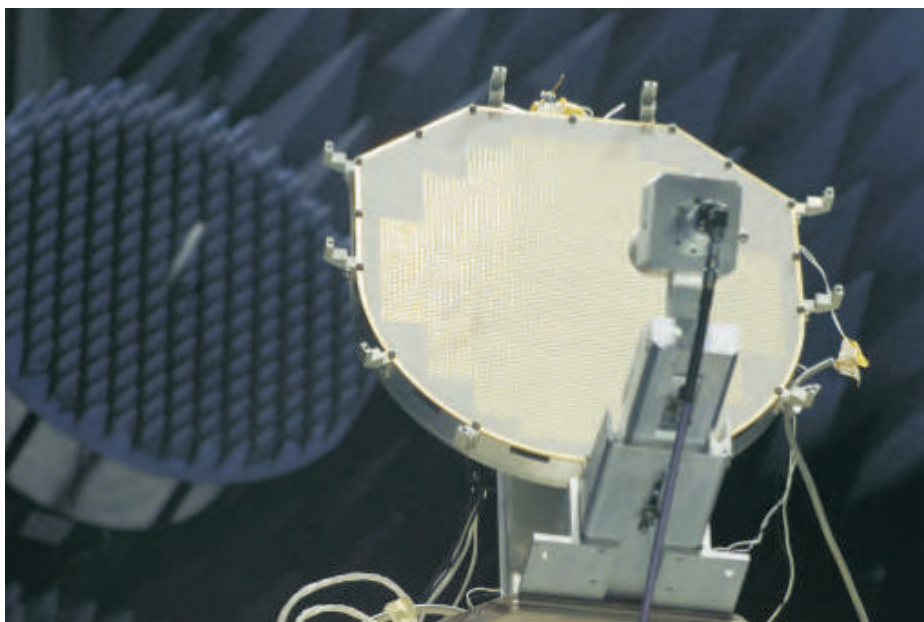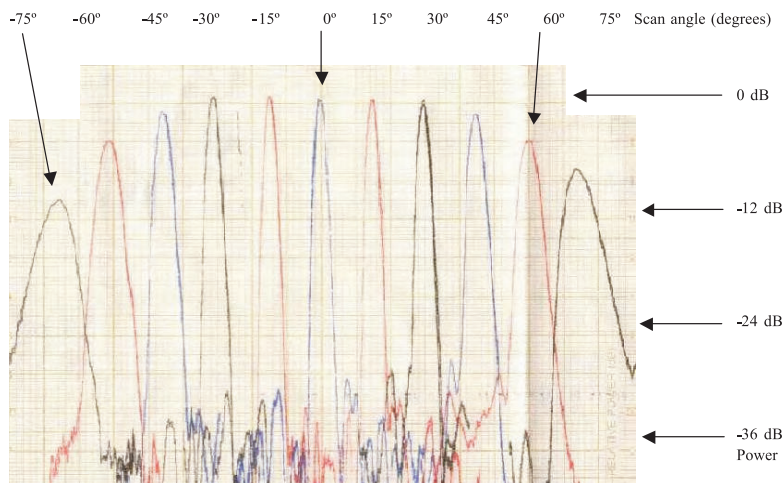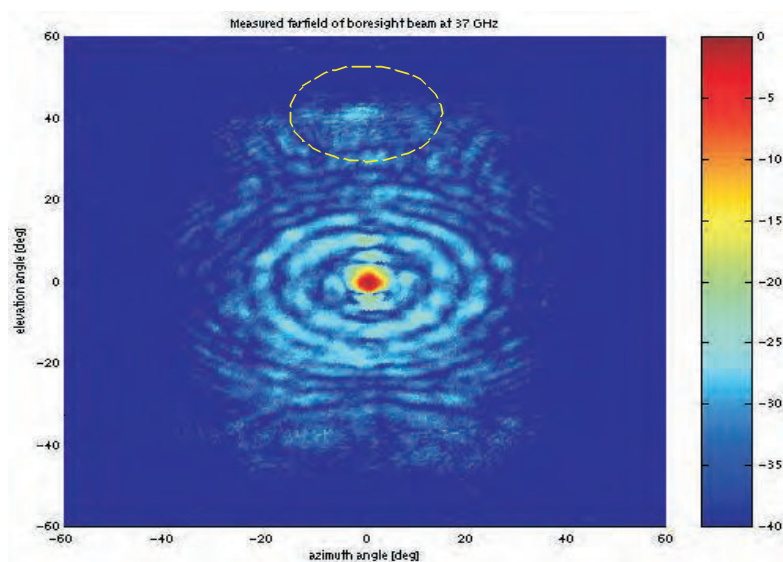
Figure 3: Response of a reflectarray sample

Figure 4: Relative power patterns electronically scanned in the azimuth plane (H-plane) covering +-75 degrees with 15-degree steps operating at 35 GHz

Figure 5 – Measured farfield of boresight beam at 37 GHz

For the reflectarray application, the multi-mode waveguide simulator is also used to improve beamforming algorithms and reduce antenna sidelobe levels.

Figure 3 shows the four phase states of the phase shifters. The best phase distribution is obtained at 35 GHz, where phase states are distributed close to uniform. The mean loss for this design is <2 dB. With these test results of the samples, the complete antenna front-end design is launched for production. The front-end reflector is first tested at digital electronics level and secondly at RF frequencies around the operational frequency band. Intermodulation products [3] are not measured. They are expected at higher harmonics of the base frequency and play a role in isolation studies.

Figure 4 presents a sequence of farfield measurements where the beam is electronically scanned from –75 to 75 degrees with 15-degree step. The horizontal scale is ±90 degrees and vertical scale is 0 to–40 dB. It shows that electronic beamsteering is working properly. Most tops of the antenna beams fairly match the theoretical cosine curve. The –75 degree beam is attenuated caused by blocking. Figure 5 shows the farfield amplitude of a boresight beam at 37 GHz. The results are from a nearfield measurement. Far-out regions are attenuated because of the limited nearfield scan plane. The region where increased sidelobe levels are expected for reflectarray antennas, the so-called direct reflection lobe (dashed), remains <-26dB. Sidelobes are mainly determined by the illumination of the reflector.

Conclusions

This paper describes the design procedure, realisation and test results of a Ka-band reflectarray demonstrator antenna. For the development of periodic RF structures such as phased array antennas and frequency selective surfaces, waveguide simulators are of major importance. The difficulty of measuring such behavior with simulators for smaller angles from boresight has been overcome using a multi-mode waveguide. The phase states of the phase shifters are distributed close to uniform and have <2 dB mean loss. Electronic beamsteering is working properly up to +-75 degrees from boresight including azimuth, elevation and the intercardinal planes. The direct reflection lobe remains < -26 dB.

References

[1] Ansoft HFSS, "Getting started: An Antenna Problem", *Ansoft Corporation,* 1994-1999

[2] John A.J. De Groot de, and Jos T.C. Duivenvoorden, "Triple-mode waveguide simulator for measurement of periodic structures and antennas", *AMTA 2001 proceedings, pp.* 153-158, October 2001

[3] W.M. Sansen, "Distortion in elementary transistor circuits", *IEEE Transactions on Circuits And Systems,* Vol. 46, pp. 315-325, March, 1999

[4] M.I. Skollnik, "Radar Handbook", *McGraw-Hill Inc.* 1990

[5] Takasu, Hideki, a.o., "Ka-band Low Loss and High Power Handling GaAs PIN Diode MMIC Phase shifter for Reflectarray-Type Phased Array Systems", *IEEE,* 1999

[6] John C. Vardaxoglou, "Frequency Selective Surfaces Analysis and Design", *John Wiley & Sons,* 1997 [7] T.K. Wu, "Frequency Selective Surfaces and Grid Array", *John Wiley & Sons Inc.,* 1995

Stelling

"Het basisprincipe van verzekeren, dat risico's door een grote groep worden gedragen, wordt onderuit gehaald door verregaande differentiatie in premies en doelgroepen"

Lukas Leyten, proefschrift:
DESIGN OF ANTENNA-DIVERSITY TRANSCEIVERS,
Technische Universiteit Eindhoven, 6 september 2002

In Memoriam Oscar Rikkert de Koe

Op 21 november l.l. overleed Oscar Rikkert de Koe, na een ziekbed van enkele weken. Hij werd geboren in 1937 en studeerde aan de Technische Universiteit Delft, alwaar hij in begin van de zestiger jaren het ingenieursdiploma behaalde bij wijlen professor Bordewijk. Na een kleine twee jaar militaire dienst, bij de Kwartiermeester Generaal (het dienstvak van de Technische Dienst), begon hij zijn carrière bij Philips op het Natuurkundig Laboratorium. Aanvankelijk werkte hij daar aan digitale transmissie, later meer aan schakelsystemen. Vanuit die periode heeft hij diverse publicaties zowel intern als internationaal (o.a. IEEE-tijdschriften) op zijn naam staan. Later ging hij werken bij Philips Telecommunicatie Industrie in Hilversum en heeft hij zijn werk voortgezet in protocollen. Hij was zeer geïnteresseerd in de nieuwste technische ontwikkelingen en gaf daar met zijn werk mede richting aan. Dit moge o.a. blijken uit het feit, dat hij in die periode mede-auteur was van het boek "Data-communicatie en Local Area Networks", en auteur van het boek "OSI-Protocollen: lagen 1 t/m 4: een inleiding tot en een beschrijving van de OSI-standaarden". Het materiaal van dit laatste boek werd ontwikkeld en beproefd in de cursus "Digitale Telecommunicatie" van de Stichting PTO van de Hogeschool van Utrecht. Hier was hij jarenlang een zeer succesvol docent. Hij was een vakman, een autoriteit van wereldklasse op zijn vakgebied, namelijk de standaardisatie van het OSI-model, de OSI-netwerklaag, HDLC en DECT.

Zijn inzet voor het NERG is haast spreekwoordelijk. Zes jaar lang, statutair de maximaal toegestane periode, was hij bestuurslid en als penningmeester verantwoordelijk voor het financiële reilen en zeilen van het NERG. Ieder die hem gekend heeft, zal begrijpen dat dit met de grootst mogelijke precisie gebeurde; het moest altijd tot op de cent

kloppen, een precisie die hij ook van zijn medebestuursleden nadrukkelijk eiste. Maar ook op beleidsterrein drukte hij in belangrijke mate zijn stempel op het NERG, altijd bereid om een extra stuk werk op zich te nemen. En wetende hoe nauwgezet hij alles wat hij toezegde ook uitvoerde, konden de overige bestuursleden dat dan ook met een gerust hart aan hem overlaten. Zo heeft hij heel veel werk verzet voor het opnieuw opzetten van onze Statuten en het Huishoudelijk Reglement in 1998. Ook voor de ledenadministratie heeft hij een volledig geautomatiseerd systeem gemaakt en vele reizen ondernomen naar Leidschendam om de administrateur in te werken, te helpen bij bijzondere problemen en het opschonen van de bestanden en de hele administratie. Dit alles ging gewoon door nadat hij geen bestuurslid meer was, puur uit enthousiasme en dienstbaarheid. Zijn verdiensten voor het NERG kunnen nauwelijks worden overschat en het NERG is aan hem dan ook veel dank verschuldigd, die we langs deze weg willen uiten.

Oscar had een vlijmscherpe geest, de wetten van de logica moesten volgens hem met uiterste precisie nageleefd worden. Discussies met hem werden op het scherpst van de snede gevoerd, maar het ging hem altijd om de zaak en hij speelde nooit op de man. Hij lokte discussie vaak ook uit, omdat hij het leuk vond, er zichtbaar van genoot. In zo'n discussie moest soms wat spanning worden weggenomen. Wie hem

goed kende, wist dat dit met een kwinkslag bij hem heel goed lukte. Middenin een heftig debat haalde hem dat zichtbaar even uit de focus op het onderwerp, zijn gezicht werd minder strak, om geleidelijk in een bulderend gelach uit barsten. Daarna kon het gesprek weer zijn loop nemen, maar was alles weer wat gerelativeerd. Deze overduidelijke aanwezigheid, zijn open, directe en enthousiaste leefwijze maakten hem een markante figuur. Diezelfde betrokkenheid kwam ook tot uiting op andere maatschappelijke terreinen waaraan hij dienstbaar was: de PHCC (Philips Hobby en Computer Club), het koor van de Händelvereniging en voor zijn vele vrienden. Reeds enige tijd had hij longproblemen, maar hij was zijn roeimaatjes dankbaar, dat ze hem desondanks volledig in de boot accepteerden. Maar ook was het zijn zorg, dat hij bij de muziekuitvoeringen teveel zou moeten hoesten.

Oscar is te vroeg van ons heengegaan. Vanwege zijn verdiensten, zijn enthousiaste openheid en betrokkenheid zullen wij in grote dankbaarheid terugdenken aan deze goede vriend. Wij wensen zijn vrouw en kinderen toe, dat zij de kracht mogen vinden om, dit voor hen ongetwijfeld smartelijke verlies, te boven te komen.

Wim van Etten
Bob van Loon
Gerard Havermans

Ledenmutaties NERG

Nieuwe leden:
Schenk, Ir. T.C.W.
    Elzenstraat 7,
    4726 BE HEERLE

Nieuwe adressen:
Braber, ir. G.P. den
    9, avenue Ledru Rollin,
    75012 PARIS,
    France

Epker, ir. H.J.
    Sint Jorisweg 21,
    3311 PK DORDRECHT
Erve, ir.ing. O.M.J. van 't
    Mozartstraat 84,
    7391 XL TWELLO
Kegel, ing. J.A.
    Ko Arnoldistraat 33,
    7558 TX HENGELO
Linden, ir. A.V.P. van de
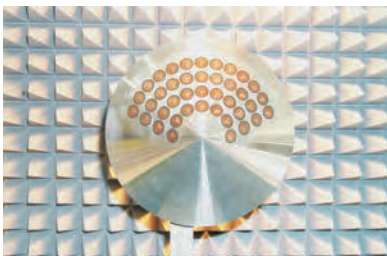   Koningsgraven 2,
    6363 BE WIJNANDSRADE

Veldhuis, ir. J.
    Thorbeckelaan 4,
    5631 AT EINDHOVEN
Zwamborn, prof.dr.ir. A.P.M.
    Bekerstraat 22,
    2492 WD 'S-GRAVENHAGE

Aankondigingen & Oproepen

c)))

3r^d European Workshop on

CONFORMAL ANTENNAS

Bonn, Germany   October 22-23, 2003

FGAN FHR

Announcement and First Call For Papers

The FGAN Research Institute for High Frequency Physics and Radar Techniques (FHR) close to Bonn, Germany, is pleased to host the 3rd European Workshop on Conformal Antennas. The Workshop is scheduled for October 22-23, 2003. The number of attendees will be limited to approximately 150. The official language of the Workshop will be English and the following topics will be addressed:

- Applications of conformal antennas
- Mathematical models and simulations
- Microstrip and waveguide antennas
- Measurement techniques
- Conformal phased and switched arrays
- Microwave and photonic feeding techniques
- Pattern synthesis

- Direction finding and adaptive conformal arrays
- Other topics concerning conformal antennas

A guided tour of the facilities of FGAN-FHR (http://www.fgan.de) is scheduled for October 24, 2003. Additional information will become available at our website or can be obtained via the conference secretary.

Information for Authors

Prospective authors are invited to submit a 400 words abstract with the name of the author, affiliation, address, phone number and e-mail address to the Conference Secretary. Abstracts are due June 2, 2003. August 4, 2003 acceptance notifications will be mailed. Authors of accepted contributions will be requested to provide a full paper (4 pages) by September 8, 2003 and give a presentation at the workshop. Early

registration is required for at least one author. Electronic submission is strongly encouraged.

Important Dates
June 2, 2003:
    400 word abstracts due
August 4, 2003:
    Notifications mailed, Opening of preregistration
September 8, 2003:
    Full papers due
October 22-23, 2003:
    Workshop
October 24, 2003:
    Tour of FGAN-FHR

Workshop Fee
The workshop fee will be approximately 120 Euro and will include proceedings, lunch and refreshments.

Bookmark
http://www.ewca-home.org

Conference Secretary:
Harald Schneider
FGAN-FHR
Neuenahrer Str. 20
D-53343 Wachtberg-Werthhoven,
Germany
Telephone: +49-228-9435-214
Telefax: +49-228-9435-521
E-mail: h.schneider@fgan.de

Conference Chairman:
Thomas Bertuch
FGAN-FHR
Neuenahrer Str. 20
D-53343 Wachtberg-Werthhoven,
Germany
Telephone: +49-228-9435-223
Telefax: +49-228-9435-521
E-mail: bertuch@fgan.de

Conference Co-Chairman:
Dr. Patrik Persson
Royal Institute of Technology Division of Electromagnetic Theory
Teknikringen 31
SE-100 44 Stockholm, Sweden
Telephone: +46-8-790-83-69
Telefax: +46-8-24-54-31
E-mail: patrik@tet.kth.se